

**Workshop on QCD
and Diffraction at LHC**

IFJ PAN

Cracow



*Probing the QCD
dynamics in
coherent
interactions*

*at
LHC*

Victor Gonçalves

UFPeI

Outline

- Motivation
- Coherent interactions (CI)
- CI as a probe of the gluon distribution
- CI as a probe of saturation: I. Vector meson production
- CI as a probe of saturation: II. Heavy quark production
- CI as a probe of the Pomeron
- CI as a probe of the BFKL Pomeron
- CI as a probe of the Odderon
- Summary

Outline

- Motivation
- Coherent interactions (CI)
- CI as a probe of the gluon distribution
- CI as a probe of saturation: I. Vector meson production
- CI as a probe of saturation: II. Heavy quark production
- CI as a probe of the Pomeron
- CI as a probe of the BFKL Pomeron
- CI as a probe of the Odderon
- Summary

Main goal: *Demonstrate that the study of coherent interactions can be useful to constrain the QCD dynamics.*

Outline

- Motivation
- Coherent interactions (CI)
- CI as a probe of the gluon distribution
- CI as a probe of saturation: I. Vector meson production
- CI as a probe of saturation: II. Heavy quark production
- CI as a probe of the Pomeron
- CI as a probe of the BFKL Pomeron
- CI as a probe of the Odderon
- Summary

Warnings: 1.) *I will skip the details of the calculations and concentrate my talk in the discussion of the results.*

Outline

- Motivation
- Coherent interactions (CI)
- CI as a probe of the gluon distribution
- CI as a probe of saturation: I. Vector meson production
- CI as a probe of saturation: II. Heavy quark production
- CI as a probe of the Pomeron
- CI as a probe of the BFKL Pomeron
- CI as a probe of the Odderon
- Summary

Warning: 2.) *I will restrict my talk in the discussion of the results obtained with my collaborators. See also important contributions to the subject by Szczurek, Schafer, Motyka and collaborators.*

Motivation



- LHC is starting its experimental program !
- Several questions remain open in the Standard Model, which will be probed in a new kinematical regime and determine the background for new physics.
- The knowledge of **QCD dynamics** at very high energies is essential in order to understand the **hadronic interactions** at current and future accelerators.
- LHC will probe gluons at very low- x , which are **not constrained** by current accelerators data.
- Although the HERA experimental results have a natural interpretation in terms of saturation physics, due to the kinematical limitations of the experiment, none of the observed phenomena (diffraction, geometric scaling, ...) can be taken as a conclusive evidence for a new regime of the QCD dynamics.
- **The study of alternatives which could constrain the QCD dynamics is timely and necessary !**

Our proposal: Study of photoproduction processes in **coherent** $pp/pA/AA$ interactions at LHC energies.

Motivation



- LHC is starting its experimental program !
- Several questions remain open in the Standard Model, which will be probed in a new kinematical regime and determine the background for new physics.
- The knowledge of **QCD dynamics** at very high energies is essential in order to understand the **hadronic interactions** at current and future accelerators.
- LHC will probe gluons at very low- x , which are **not constrained** by current accelerators data.
- Although the HERA experimental results have a natural interpretation in terms of saturation physics, due to the kinematical limitations of the experiment, none of the observed phenomena (diffraction, geometric scaling, ...) can be taken as a conclusive evidence for a new regime of the QCD dynamics.
- **The study of alternatives which could constrain the QCD dynamics is timely and necessary !**

Our proposal: Study of photoproduction processes in **coherent** $pp/pA/AA$ interactions at LHC energies.

Motivation



- LHC is starting its experimental program !
- Several questions remain open in the Standard Model, which will be probed in a new kinematical regime and determine the background for new physics.
- The knowledge of **QCD dynamics** at very high energies is essential in order to understand the **hadronic interactions** at current and future accelerators.
- LHC will probe gluons at very low- x , which are **not constrained** by current accelerators data.
- Although the HERA experimental results have a natural interpretation in terms of saturation physics, due to the kinematical limitations of the experiment, none of the observed phenomena (diffraction, geometric scaling, ...) can be taken as a conclusive evidence for a new regime of the QCD dynamics.
- **The study of alternatives which could constrain the QCD dynamics is timely and necessary !**

Our proposal: Study of photoproduction processes in **coherent** $pp/pA/AA$ interactions at LHC energies.

Motivation

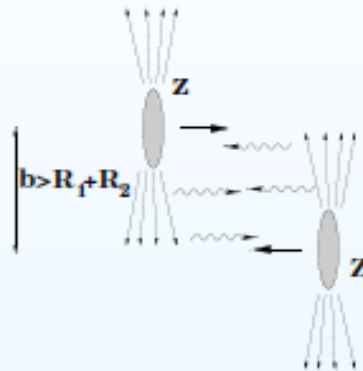


- LHC is starting its experimental program !
- Several questions remain open in the Standard Model, which will be probed in a new kinematical regime and determine the background for new physics.
- The knowledge of **QCD dynamics** at very high energies is essential in order to understand the **hadronic interactions** at current and future accelerators.
- LHC will probe gluons at very low- x , which are **not constrained** by current accelerators data.
- Although the HERA experimental results have a natural interpretation in terms of saturation physics, due to the kinematical limitations of the experiment, none of the observed phenomena (diffraction, geometric scaling, ...) can be taken as a conclusive evidence for a new regime of the QCD dynamics.
- **The study of alternatives which could constrain the QCD dynamics is timely and necessary !**

Our proposal: Study of photoproduction processes in **coherent** $pp/pA/AA$ interactions at LHC energies.

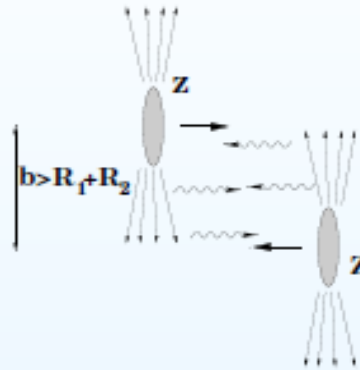
Coherent interactions

- Protons/ions at collider energies are a source of high-energy Weizsäcker-Williams photons.



Coherent interactions

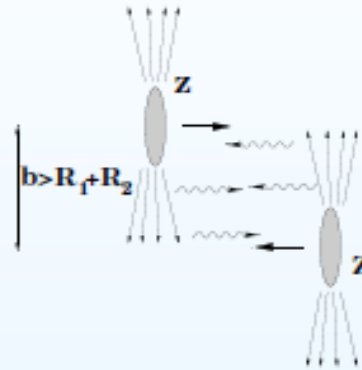
- Protons/ions at collider energies are a source of high-energy Weizsäcker-Williams photons.



- The coherence condition limits the photon virtuality to very low values $Q^2 \leq 1/R^2$, where R is the radius of the hadron. $\Rightarrow Q^2 \approx 0$!

Coherent interactions

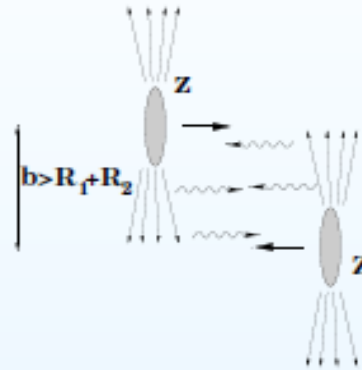
- Protons/ions at collider energies are a source of high-energy Weizsäcker-Williams photons.



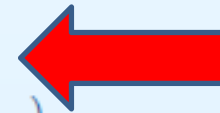
- The coherence condition limits the photon virtuality to very low values $Q^2 \leq 1/R^2$, where R is the radius of the hadron. $\Rightarrow Q^2 \approx 0$!
- At large impact parameter ($b > R_1 + R_2$) the electromagnetic interaction is dominant. One can study:
 - γh Processes: $\sigma(h_1 h_2 \rightarrow X) = n_h(\omega) \otimes \sigma^{\gamma h \rightarrow X}(W_{\gamma h})$
 - $\gamma\gamma$ Processes: $\sigma(h_1 h_2 \rightarrow X) = n_1(\omega) \otimes n_2(\omega) \otimes \sigma^{\gamma\gamma \rightarrow X}(W_{\gamma\gamma})$

Coherent interactions

- Protons/ions at collider energies are a source of high-energy Weizsäcker-Williams photons.



- The coherence condition limits the photon virtuality to very low values $Q^2 \leq 1/R^2$, where R is the radius of the hadron. $\Rightarrow Q^2 \approx 0!$
- At large impact parameter ($b > R_1 + R_2$) the electromagnetic interaction is dominant. One can study:
 - γh Processes: $\sigma(h_1 h_2 \rightarrow X) = n_h(\omega) \otimes \sigma^{\gamma h \rightarrow X}(W_{\gamma h})$
 - $\gamma\gamma$ Processes: $\sigma(h_1 h_2 \rightarrow X) = n_1(\omega) \otimes n_2(\omega) \otimes \sigma^{\gamma\gamma \rightarrow X}(W_{\gamma\gamma})$



Coherent interactions

Center of mass energies

LHC	pp	$W_{\gamma p} \lesssim 8390 \text{ GeV}$	$W_{\gamma\gamma} \lesssim 4504 \text{ GeV}$
LHC	$pPb(Ar)$	$W_{\gamma A} \lesssim 1500 (2130) \text{ GeV}$	$W_{\gamma\gamma} \lesssim 260 (480) \text{ GeV}$
LHC	$PbPb$	$W_{\gamma A} \lesssim 950 \text{ GeV}$	$W_{\gamma\gamma} \lesssim 160 \text{ GeV}$
HERA	ep	$W_{\gamma p} \lesssim 200 \text{ GeV}$	–

Coherent interactions

Center of mass energies

LHC	pp	$W_{\gamma p} \lesssim 8390 \text{ GeV}$	$W_{\gamma\gamma} \lesssim 4504 \text{ GeV}$
LHC	$pPb(Ar)$	$W_{\gamma A} \lesssim 1500 (2130) \text{ GeV}$	$W_{\gamma\gamma} \lesssim 260 (480) \text{ GeV}$
LHC	$PbPb$	$W_{\gamma A} \lesssim 950 \text{ GeV}$	$W_{\gamma\gamma} \lesssim 160 \text{ GeV}$
HERA	ep	$W_{\gamma p} \lesssim 200 \text{ GeV}$	–

Photoproduction in coherent interactions can help us to gain information on the QCD Dynamics for energies higher than HERA.

Photoproduction cross section

- The photoproduction cross section is given by,

$$\sigma(h_1 h_2 \rightarrow X)(\sqrt{s}) = \int \frac{d\omega}{\omega} n_h(\omega) \sigma_{\gamma h}(W_{\gamma h}^2 = 2\omega\sqrt{s})$$

- The number of equivalent photons:

$$n_A(\omega) = \frac{2Z^2\alpha_{em}}{\pi\omega} \left[\bar{\eta} K_0(\bar{\eta}) K_1(\bar{\eta}) + \frac{\bar{\eta}^2}{2} (K_1^2(\bar{\eta}) - K_0^2(\bar{\eta})) \right],$$

where $\bar{\eta} = \omega R_{eff}/\gamma_L$, with $R_{eff} = R_p + R_A$ ($R_{eff} = 2R_A$) for pA (AA) collisions.

$$n_p(\omega) = \frac{\alpha_{em}}{2\pi\omega} \left[1 + \left(1 - \frac{2\omega}{\sqrt{S_{NN}}} \right)^2 \right] \left(\ln \Omega - \frac{11}{6} + \frac{3}{\Omega} - \frac{3}{2\Omega^2} + \frac{1}{3\Omega^3} \right),$$

where $\Omega = 1 + [(0.71 \text{ GeV}^2)/Q_{\min}^2]$ and $Q_{\min}^2 = \omega^2/[\gamma_L^2 (1 - 2\omega/\sqrt{s})]$.

Photoproduction cross section

- The photoproduction cross section is given by,



$$\sigma(h_1 h_2 \rightarrow X)(\sqrt{s}) = \int \frac{d\omega}{\omega} n_h(\omega) \sigma_{\gamma h}(W_{\gamma h}^2 = 2\omega\sqrt{s})$$

- The number of equivalent photons:

$$n_A(\omega) = \frac{2Z^2\alpha_{em}}{\pi\omega} \left[\bar{\eta} K_0(\bar{\eta}) K_1(\bar{\eta}) + \frac{\bar{\eta}^2}{2} (K_1^2(\bar{\eta}) - K_0^2(\bar{\eta})) \right],$$

where $\bar{\eta} = \omega R_{eff}/\gamma_L$, with $R_{eff} = R_p + R_A$ ($R_{eff} = 2R_A$) for pA (AA) collisions.

$$n_p(\omega) = \frac{\alpha_{em}}{2\pi\omega} \left[1 + \left(1 - \frac{2\omega}{\sqrt{S_{NN}}} \right)^2 \right] \left(\ln \Omega - \frac{11}{6} + \frac{3}{\Omega} - \frac{3}{2\Omega^2} + \frac{1}{3\Omega^3} \right),$$

where $\Omega = 1 + [(0.71 \text{ GeV}^2)/Q_{min}^2]$ and $Q_{min}^2 = \omega^2/[\gamma_L^2 (1 - 2\omega/\sqrt{s})]$.

Inclusive and exclusive processes

We focus our study in processes which can be calculated using perturbative QCD, which can be classified as:

- **Inclusive processes:** $\gamma p \rightarrow XY$

\Rightarrow Heavy quark photoproduction ($X = c\bar{c}, b\bar{b}$)

The final state is characterized by **one rapidity gap** due to the dissociation of the hadron target ($pp \rightarrow p \otimes XY$).

- **Exclusive processes:** $\gamma p \rightarrow Xp$

\Rightarrow Heavy vector meson photoproduction ($X = J/\Psi, \Upsilon$)

The final state is characterized by **two rapidity gaps**
($pp \rightarrow p \otimes X \otimes p$).

Coherent interactions as a probe of the gluon distribution

PHYSICAL REVIEW C, VOLUME 65, 054905

Peripheral heavy ion collisions as a probe of the nuclear gluon distribution

V. P. Gonçalves^{1,*} and C. A. Bertulani^{2,†}

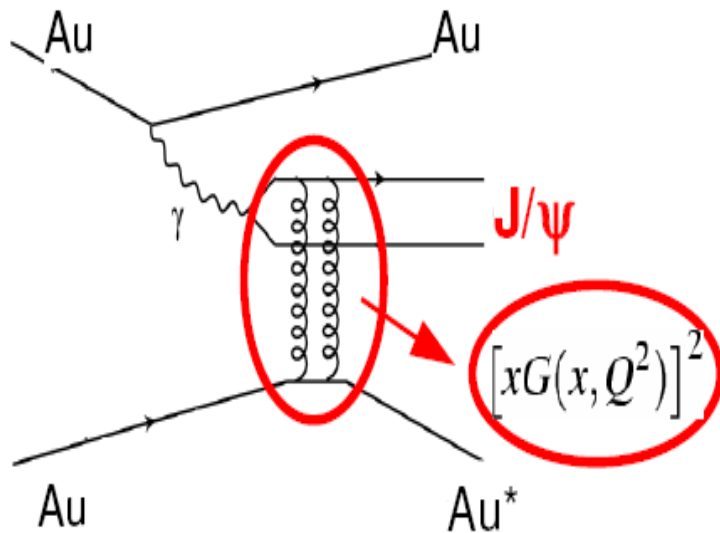
¹*Instituto de Física e Matemática, Universidade Federal de Pelotas, Caixa Postal 354, CEP 96010-090, Pelotas, RS, Brazil*

²*Department of Physics and Astronomy and National Superconducting Cyclotron Laboratory, Michigan State University, East Lansing, Michigan 48824-1321*

(Received 29 October 2001; published 29 April 2002)

At high energies a quark-gluon plasma is expected to be formed in heavy-ion collisions at the Relativistic Heavy-Ion Collider and the Large Hadron Collider. The theoretical description of these processes is directly associated to a complete knowledge of the details of medium effects in the nuclear gluon distribution. In this paper we analyze the possibility to constrain the behavior of this distribution considering peripheral heavy ion collisions. We reanalyze the photoproduction of heavy quarks for the deduction of the in-medium gluon distribution using three current parametrizations for this parton distribution. Moreover we show that the elastic photoproduction of vector mesons is a potential process to probe the nuclear gluon distribution.

Coherent interactions as a probe of the gluon distribution



$$\frac{d\sigma [A + A \rightarrow A \otimes V \otimes A]}{dY} = \omega \frac{dN_\gamma(\omega)}{d\omega} \sigma_{\gamma A \rightarrow V A}(\omega)$$

$$\sigma(\gamma p \rightarrow V p) = \frac{1}{b} \frac{d\sigma(\gamma h \rightarrow V h)}{dt} \Big|_{t=0}$$

$$\frac{d\sigma(\gamma h \rightarrow V h)}{dt} = \frac{\pi^3 \Gamma_{ee} M_V^3}{48\alpha} \frac{\alpha_s^2(\bar{Q}^2)}{\bar{Q}^8} \times [xg_h(x, \bar{Q}^2)]^2$$

$$x = 4\bar{Q}^2/W^2$$

$$\bar{Q}^2 = M_V^2/4$$

Nuclear shadowing from exclusive quarkonium photoproduction at the BNL Relativistic Heavy Ion Collider (RHIC) and the CERN Large Hadron Collider (LHC)

A. L. Ayala Filho, V. P. Gonçalves, and M. T. Griep

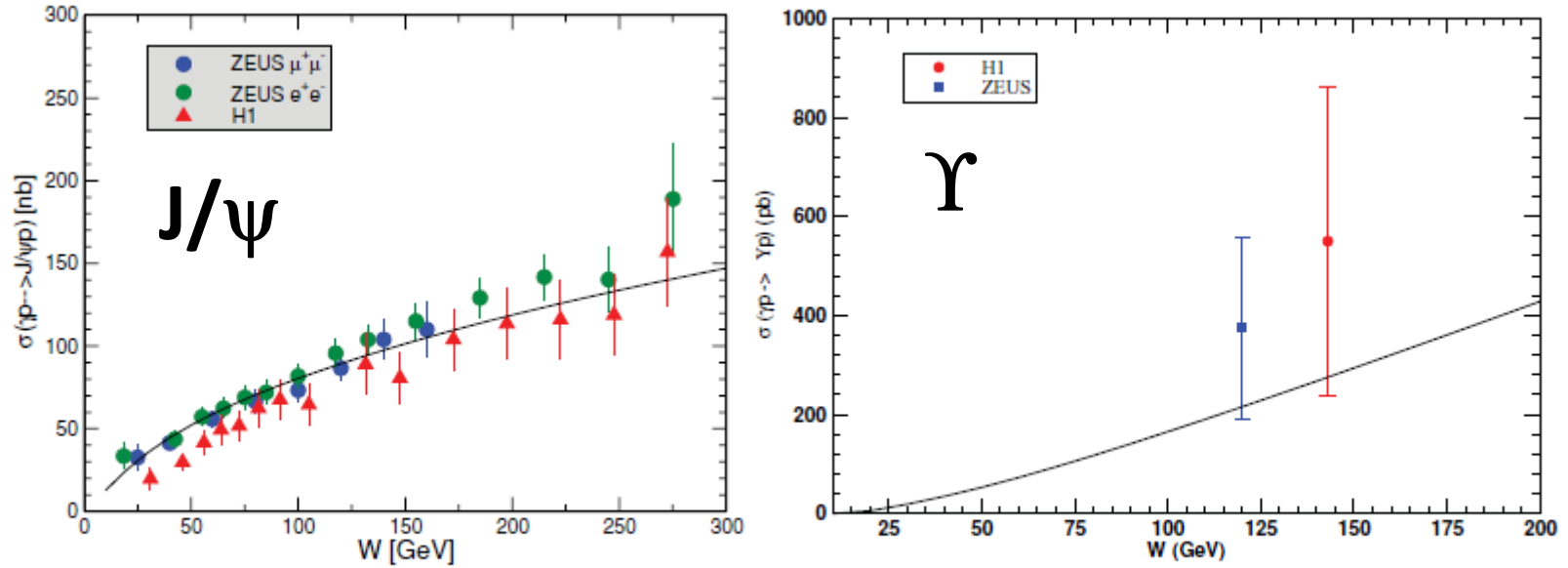
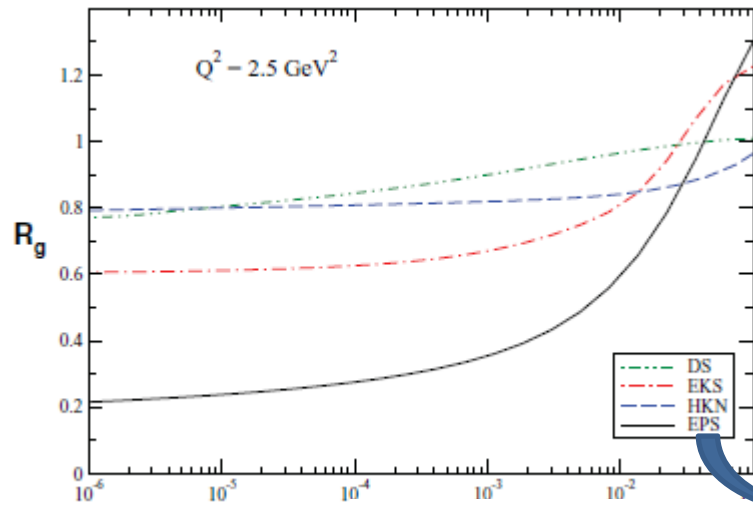


FIG. 1. (Color online) Energy dependence of the exclusive J/ψ (left panel) and Υ (right panel) photoproduction cross sections. Comparison with HERA data [35–37].

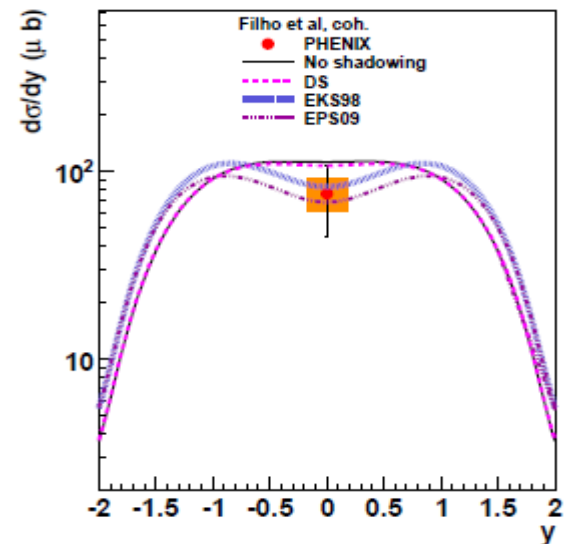
Nuclear effects in the gluon distribution:

$$R_g \equiv xg_A / A \cdot \bar{x}g_N$$



Solutions of the
linear DGLAP
evolution equations

PHENIX result:



Predictions at LHC

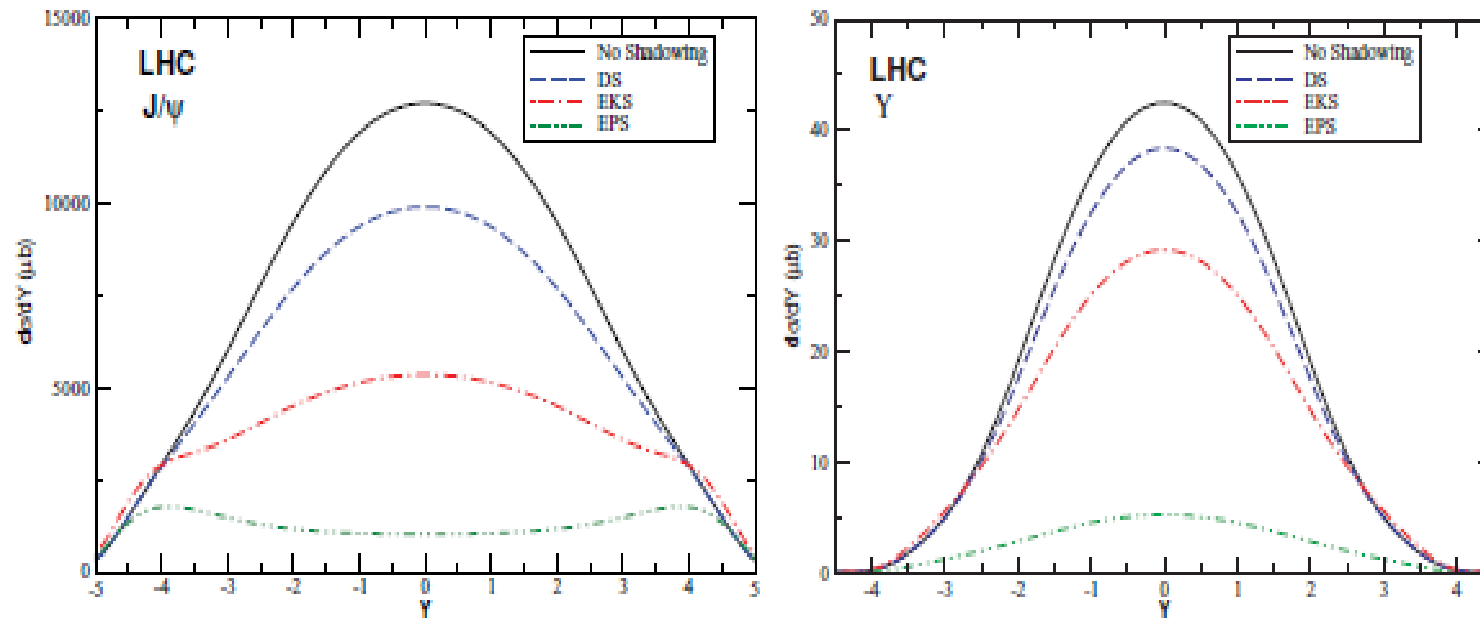


FIG. 4. (Color online) The rapidity distribution for nuclear vector meson photoproduction on UPCs in AA reactions at LHC energy ($\sqrt{s_{NN}} = 5.5$ TeV).

Predictions at LHC

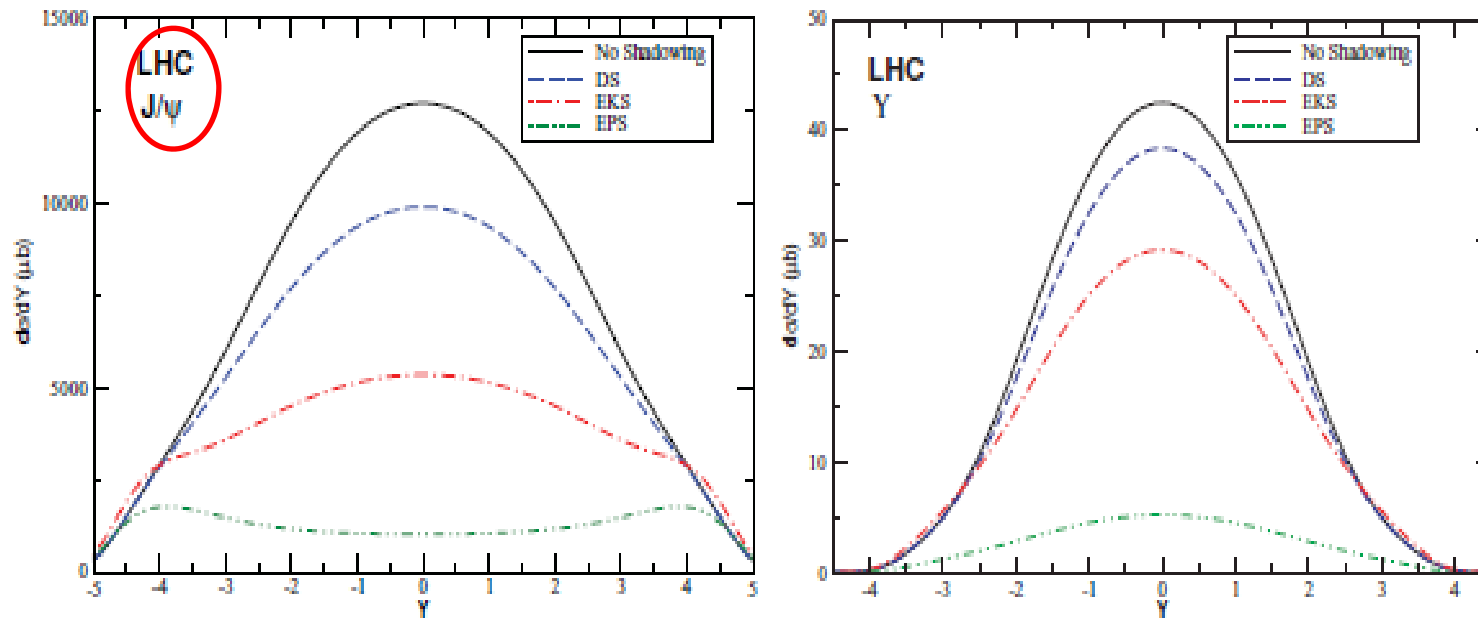


FIG. 4. (Color online) The rapidity distribution for nuclear vector meson photoproduction on UPCs in AA reactions at LHC energy ($\sqrt{s_{NN}} = 5.5 \text{ TeV}$).

Predictions at LHC

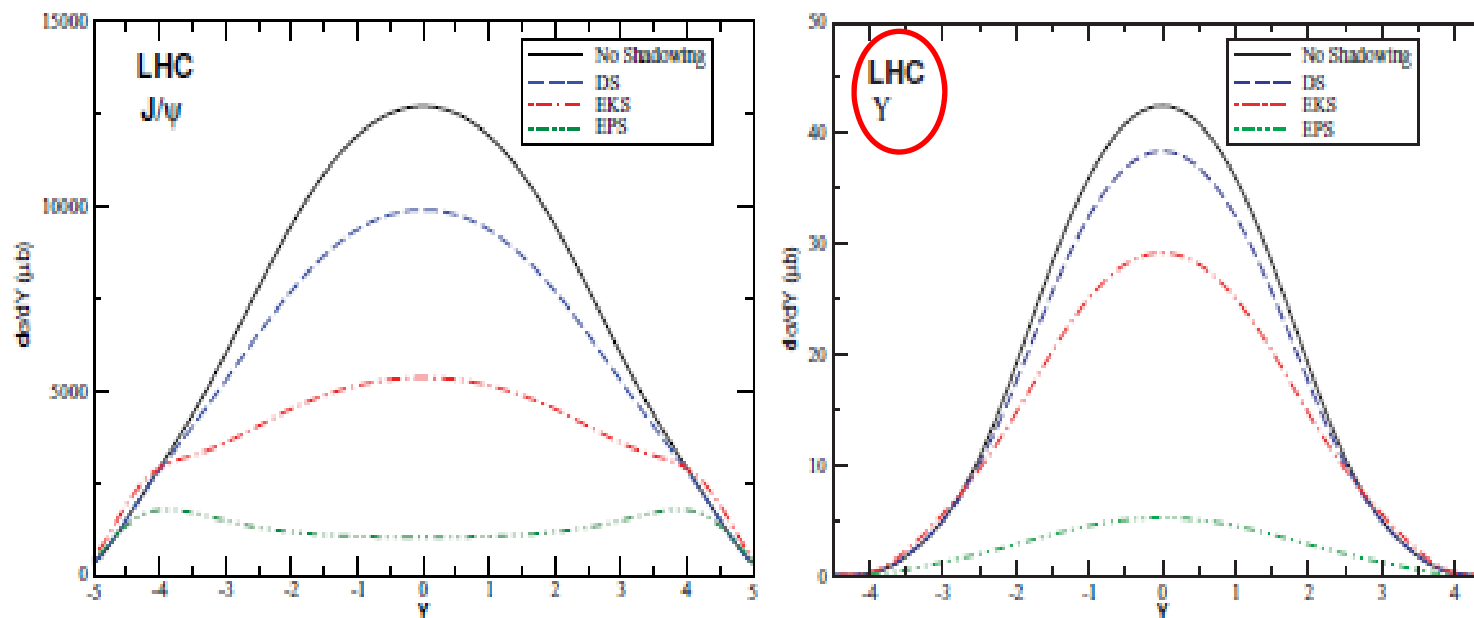


FIG. 4. (Color online) The rapidity distribution for nuclear vector meson photoproduction on UPCs in AA reactions at LHC energy ($\sqrt{s_{NN}} = 5.5 \text{ TeV}$).

Predictions at LHC

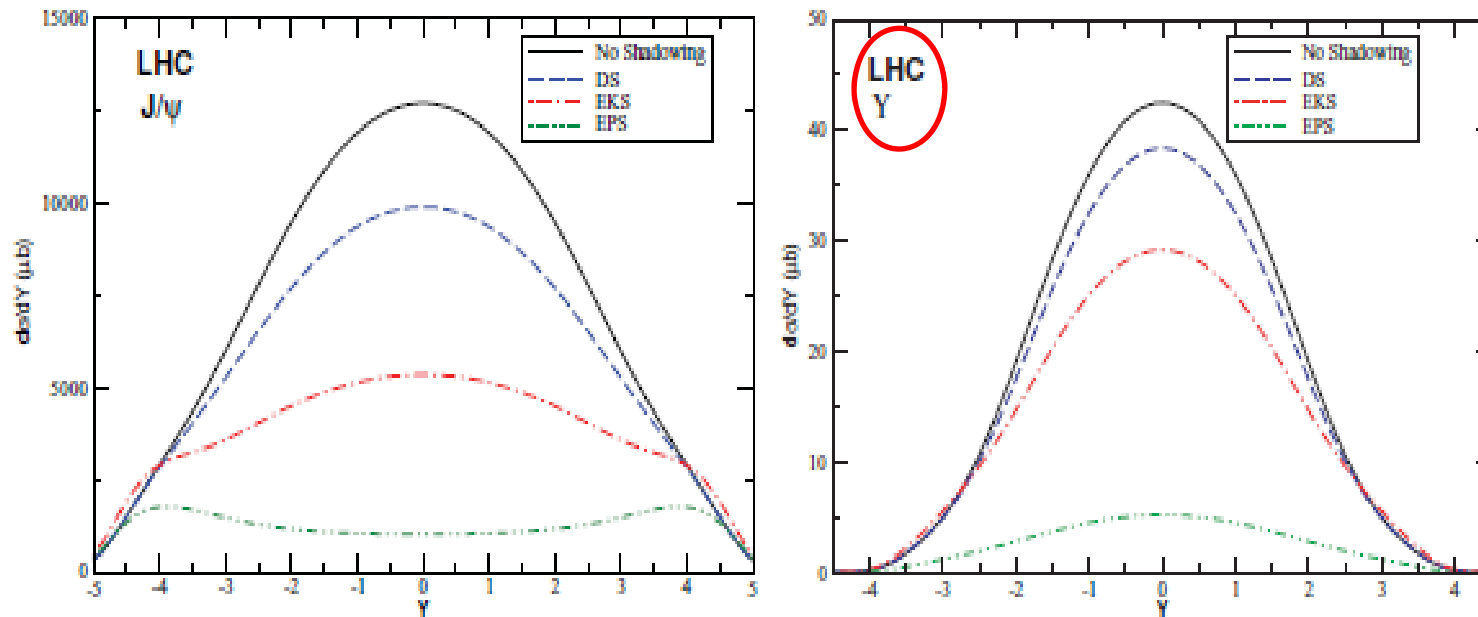
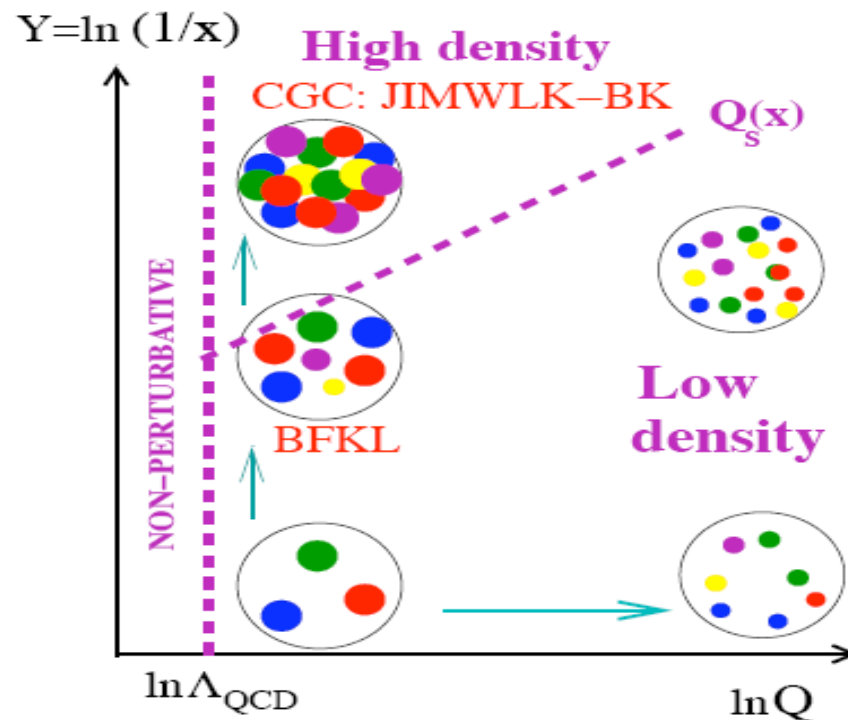


FIG. 4. (Color online) The rapidity distribution for nuclear vector meson photoproduction on UPCs in AA reactions at LHC energy ($\sqrt{s_{NN}} = 5.5 \text{ TeV}$).

Shortcoming: *LT analysis that disregard non-linear effects in the QCD dynamics.*

QCD dynamics at high energies



⇒ **Saturation:** At small Bjorken- x the hadron wave function gets dense and non-linear processes become a relevant dynamical ingredient

Coherent interactions as a probe of the saturation: I. Vector Meson Production

Eur. Phys. J. C 40, 519–529 (2005)
Digital Object Identifier (DOI) 10.1140/epjc/s2005-02175-3

THE EUROPEAN
PHYSICAL JOURNAL C

The QCD pomeron in ultraperipheral heavy ion collisions: IV. Photonuclear production of vector mesons

V.P. Gonçalves¹, M.V.T. Machado^{2,3,a}

¹ Instituto de Física e Matemática, Universidade Federal de Pelotas, Caixa Postal 354, CEP 96010-090, Pelotas, RS, Brazil

² Universidade Estadual do Rio Grande do Sul – UERGS, Unidade de Bento Gonçalves, CEP 95700-000, Bento Gonçalves, RS, Brazil

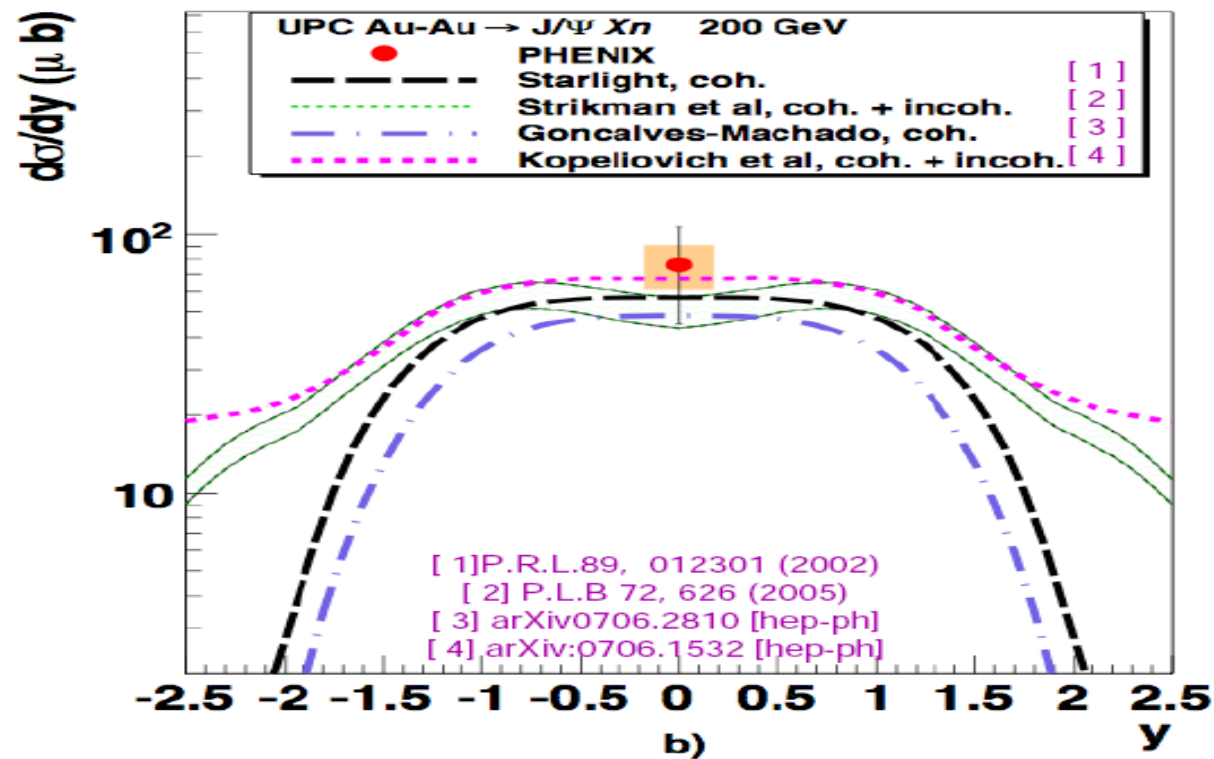
³ High Energy Physics Phenomenology Group, GFPAE IF-UFRGS, Caixa Postal 15051, CEP 91501-970, Porto Alegre, RS, Brazil

Received: 12 January 2005 / Revised version: 2 February 2005 /

Published online: 9 March 2005 – © Springer-Verlag / Società Italiana di Fisica 2005

Abstract. The photonuclear production of vector mesons in ultraperipheral heavy-ion collisions is investigated within the QCD color dipole picture, with particular emphasis on the saturation model. The integrated cross section and the rapidity distribution for the $AA \rightarrow V AA$ ($V = \rho, \omega, \phi, J/\Psi$) process are computed and theoretical estimates for scattering on both light and heavy nuclei are given for the energies of RHIC and LHC. A comparison with the recent STAR data on coherent production of ρ mesons is also presented. Furthermore, we calculate the photoproduction of vector mesons in proton–proton collisions at RHIC, Tevatron and LHC energies.

Exclusive J/ψ photoproduction at RHIC



**Phenix Collaboration
PLB679 (2009) 321*

Exclusive J/ψ photoproduction at Tevatron

PRL 102, 242001 (2009)

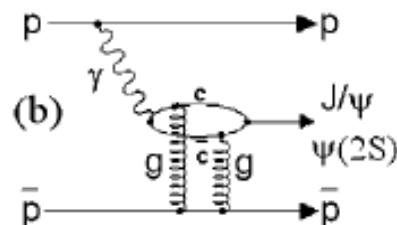
PHYSICAL REVIEW LETTERS

week ending
19 JUNE 2009

Observation of Exclusive Charmonium Production and $\gamma\gamma \rightarrow \mu^+\mu^-$ in $p\bar{p}$ Collisions at $\sqrt{s} = 1.96$ TeV

(CDF Collaboration)

In CDF we have observed the reactions $p + \bar{p} \rightarrow p + X + \bar{p}$, with X being a centrally produced J/ψ , $\psi(2S)$, or χ_{c0} , and $\gamma\gamma \rightarrow \mu^+\mu^-$ in $p\bar{p}$ collisions at $\sqrt{s} = 1.96$ TeV. The event signature requires two oppositely charged central muons, and either no other particles or one additional photon detected. Exclusive vector meson production is as expected for elastic photoproduction, $\gamma + p \rightarrow J/\psi(\psi(2S)) + p$, observed here for the first time in hadron-hadron collisions. We also observe exclusive $\chi_{c0} \rightarrow J/\psi + \gamma$. The cross sections $\frac{d\sigma}{dy}|_{y=0}$ for J/ψ , $\psi(2S)$, and χ_{c0} are $3.92 \pm 0.25(\text{stat}) \pm 0.52(\text{syst})$ nb, $0.53 \pm 0.09(\text{stat}) \pm 0.10(\text{syst})$ nb, and $76 \pm 10(\text{stat}) \pm 10(\text{syst})$ nb, respectively, and the continuum is consistent with QED. We put an upper limit on the cross section for Odderon exchange in exclusive J/ψ production.



Our prediction:* 3.4 nb

**VPG and Machado, EPJC40 (2005)519*

Exclusive ρ photoproduction

PHYSICAL REVIEW C 80, 054901 (2009)

Photoproduction of ρ^0 mesons in ultraperipheral heavy ion collisions at energies available at the BNL Relativistic Heavy Ion Collider (RHIC) and CERN Large Hadron Collider (LHC)

V. P. Gonçalves^{1,*} and M. V. T. Machado²

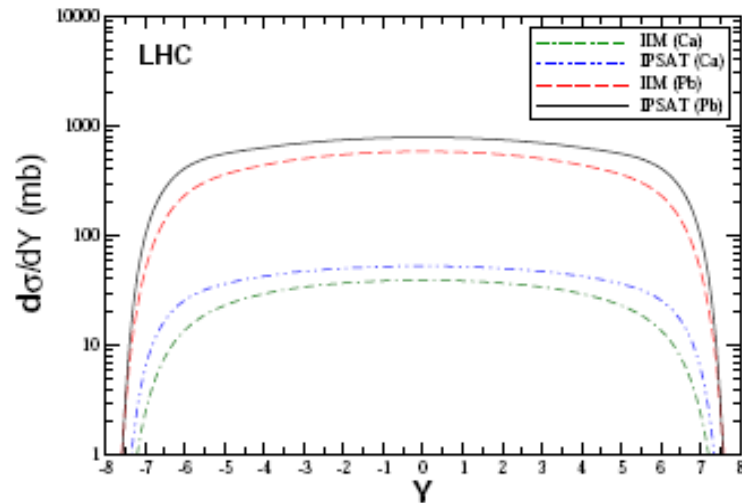


FIG. 4: (Color online) Predictions for the rapidity distribution of ρ^0 photoproduction in PbPb and CaCa collisions at the LHC. The results for IP-SAT and IIM models are presented.

A	IIM	IP-SAT
Ca	395 mb (16985.0)	572 mb (24600.0)
Pb	5977 mb (2510.0)	8596 mb (3610.0)

TABLE I: The integrated cross section (events rate/second) for the ρ^0 photoproduction in AA collisions at LHC energies and different nuclei ($A = \text{Pb}$ and Ca).

Exclusive ρ photoproduction

PHYSICAL REVIEW C 80, 054901 (2009)

Photoproduction of ρ^0 mesons in ultraperipheral heavy ion collisions at energies available at the BNL Relativistic Heavy Ion Collider (RHIC) and CERN Large Hadron Collider (LHC)

V. P. Gonçalves^{1,*} and M. V. T. Machado²

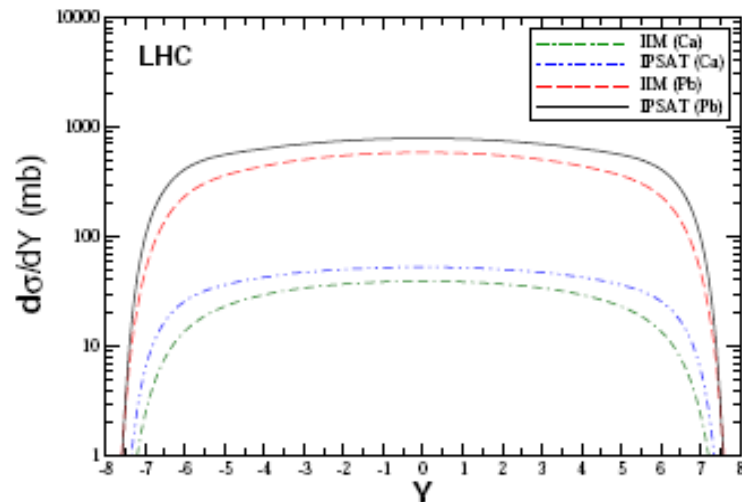
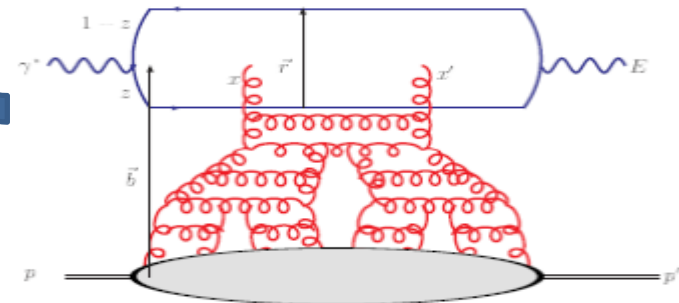


FIG. 4: (Color online) Predictions for the rapidity distribution of ρ^0 photoproduction in PbPb and CaCa collisions at the LHC. The results for IP-SAT and IIM models are presented.

A	IIM	IP-SAT
Ca	395 mb (16985.0)	572 mb (24600.0)
Pb	5977 mb (2510.0)	8596 mb (3610.0)

TABLE I: The integrated cross section (events rate/second) for the ρ^0 photoproduction in AA collisions at LHC energies and different nuclei ($A = \text{Pb}$ and Ca).



Exclusive ρ photoproduction

PHYSICAL REVIEW C 80, 054901 (2009)

Photoproduction of ρ^0 mesons in ultraperipheral heavy ion collisions at energies available at the BNL Relativistic Heavy Ion Collider (RHIC) and CERN Large Hadron Collider (LHC)

V. P. Gonçalves^{1,*} and M. V. T. Machado²

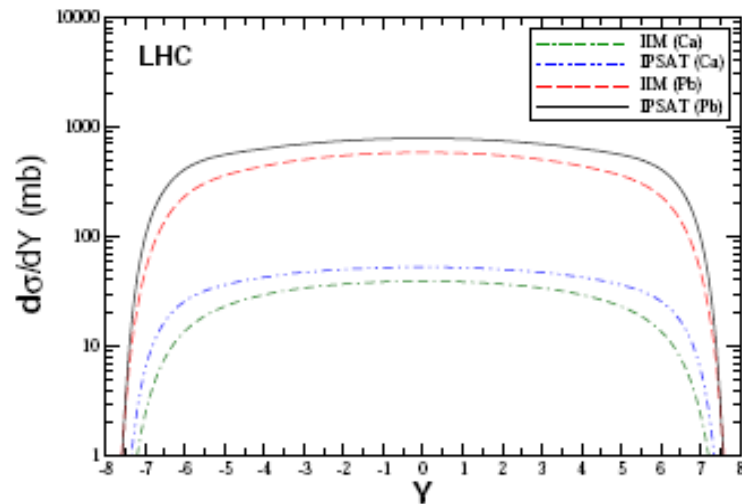
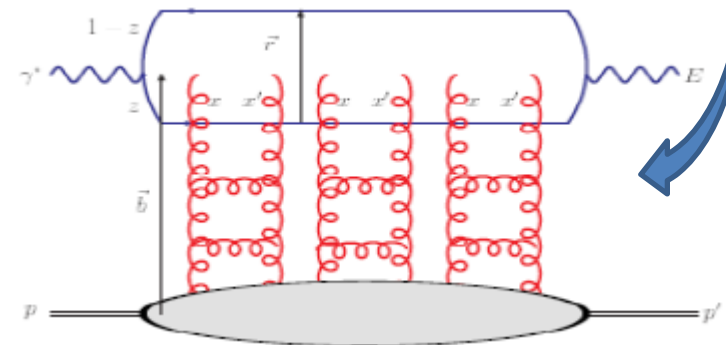


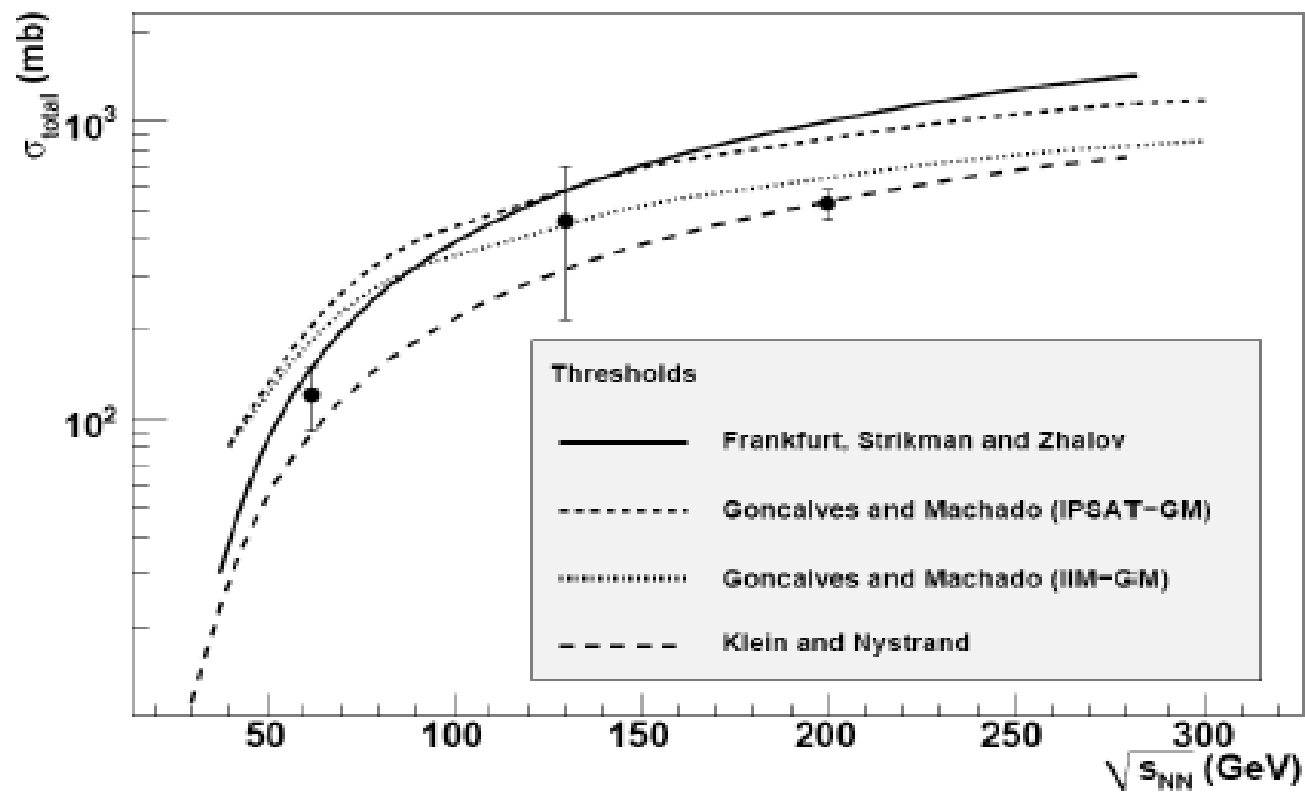
FIG. 4: (Color online) Predictions for the rapidity distribution of ρ^0 photoproduction in PbPb and CaCa collisions at the LHC. The results for IP-SAT and IIM models are presented.

A	IIM	IP-SAT
Ca	395 mb (16985.0)	572 mb (24600.0)
Pb	5977 mb (2510.0)	8596 mb (3610.0)

TABLE I: The integrated cross section (events rate/second) for the ρ^0 photoproduction in AA collisions at LHC energies and different nuclei ($A = \text{Pb}$ and Ca).



Star collaboration results:



Update on predictions for the first LHC run:

PHYSICAL REVIEW C 84, 011902(R) (2011)

Vector meson production in coherent hadronic interactions: Update on predictions for energies available at the BNL Relativistic Heavy Ion Collider and the CERN Large Hadron Collider

V. P. Gonçalves¹ and M. V. T. Machado²

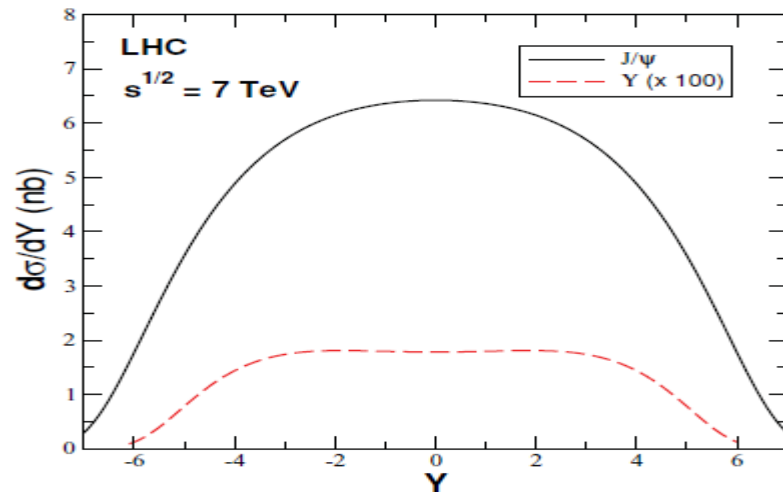


FIG. 1. (Color online) Predictions for the rapidity distribution of J/ψ and Υ photoproduction in pp collisions at LHC ($\sqrt{s} = 7$ TeV).

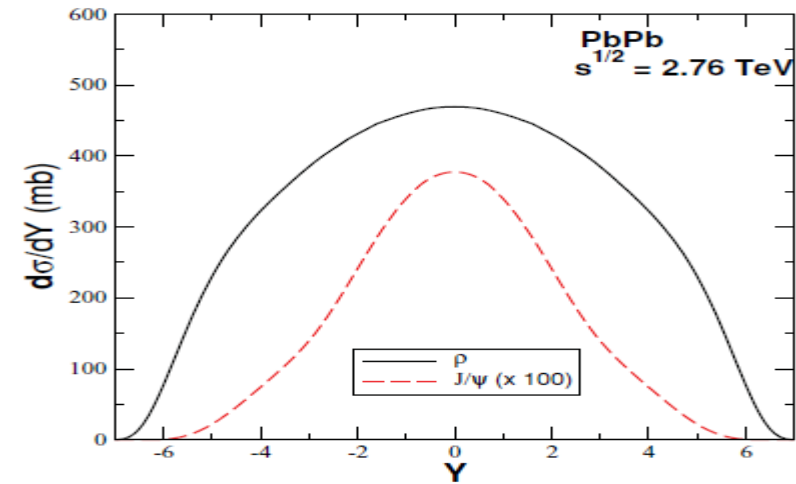


FIG. 3. (Color online) Predictions for the rapidity distribution of ρ and J/ψ photoproduction in $PbPb$ collisions at LHC.

TABLE I. The integrated cross section (events rate/second) for vector meson photoproduction in pp and AA collisions at RHIC and LHC energies.

Meson	RHIC ($AuAu$)	LHC ($PbPb$)	LHC (pp)
ρ	609.7 mb (256.0)	4276 mb (1796.0)	—
J/ψ	0.51 mb (0.20)	20 mb (8.40)	63.70 nb (637.0)
Υ	—	—	0.18 nb (1.80)

Coherent interactions as a probe of the saturation: II. Heavy quark production

Eur. Phys. J. C 31, 371–378 (2003)
Digital Object Identifier (DOI) 10.1140/epjc/s2003-01348-4

THE EUROPEAN
PHYSICAL JOURNAL C

The QCD pomeron in ultraperipheral heavy ion collisions: III. Photonuclear production of heavy quarks

V.P. Gonçalves¹, M.V.T. Machado^{1,2}

¹ Instituto de Física e Matemática, Universidade Federal de Pelotas, Caixa Postal 354, CEP 96010-090, Pelotas, RS, Brazil

² High Energy Physics Phenomenology Group, GFPAE, IF-UFRGS, Caixa Postal 15051, CEP 91501-970, Porto Alegre, RS, Brazil

Received: 11 August 2003 / Revised version: 3 September 2003 /

Published online: 10 October 2003 – © Springer-Verlag / Società Italiana di Fisica 2003

Abstract. We calculate the photonuclear production of heavy quarks in ultraperipheral heavy ion collisions. The integrated cross section and the rapidity distribution are computed employing sound high energy QCD formalisms like the collinear and semihard approaches as well as the saturation model. In particular, the color glass condensate (CGC) formalism is also considered using a simple phenomenological parameterization for the color field correlator in the medium, which allows us to obtain more reliable estimates for charm and bottom production at LHC energies.

Heavy quark photoproduction in coherent interactions at high energies

V. P. Gonçalves,¹ M. V. T. Machado,² and A. R. Meneses¹

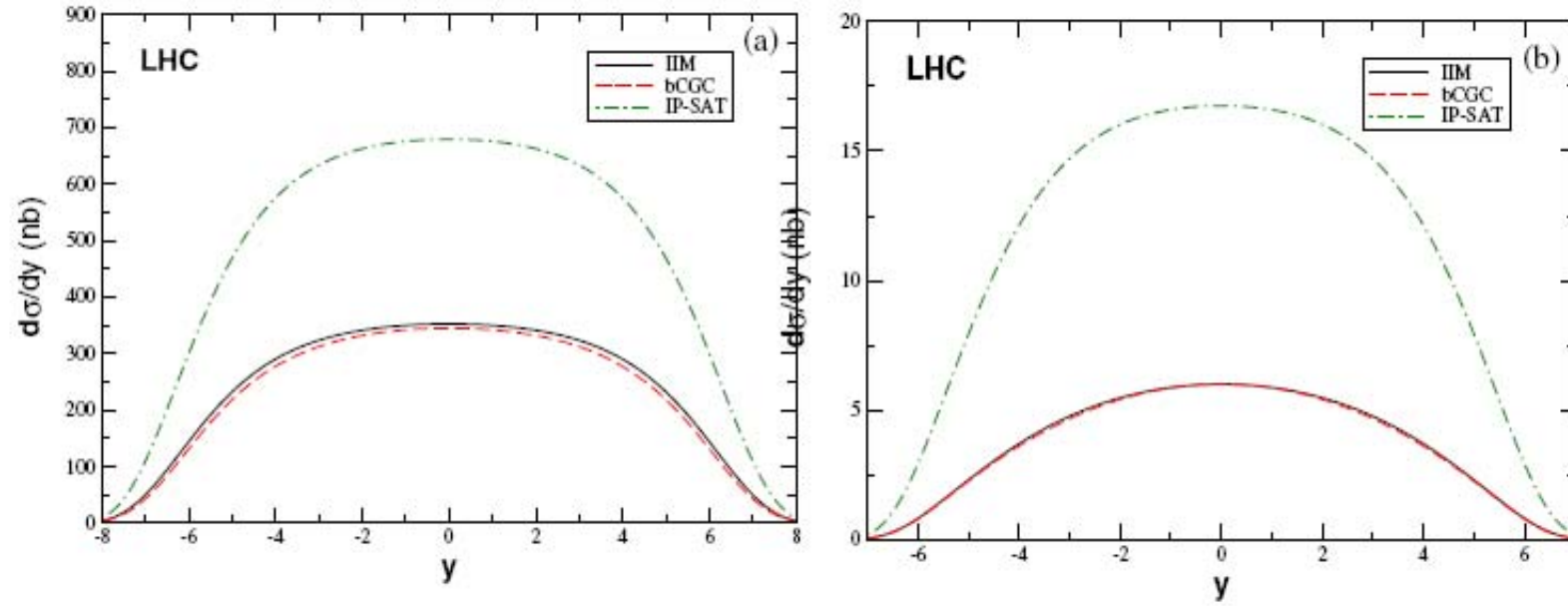


FIG. 5 (color online). The rapidity distribution for the inclusive charm (left panel) and bottom (right panel) photoproduction on $p\bar{p}$ reactions at LHC energy $\sqrt{s_{NN}} = 14$ TeV. Different curves correspond to distinct phenomenological models.

Heavy quark photoproduction in coherent interactions at high energies

V. P. Gonçalves,¹ M. V. T. Machado,² and A. R. Meneses¹

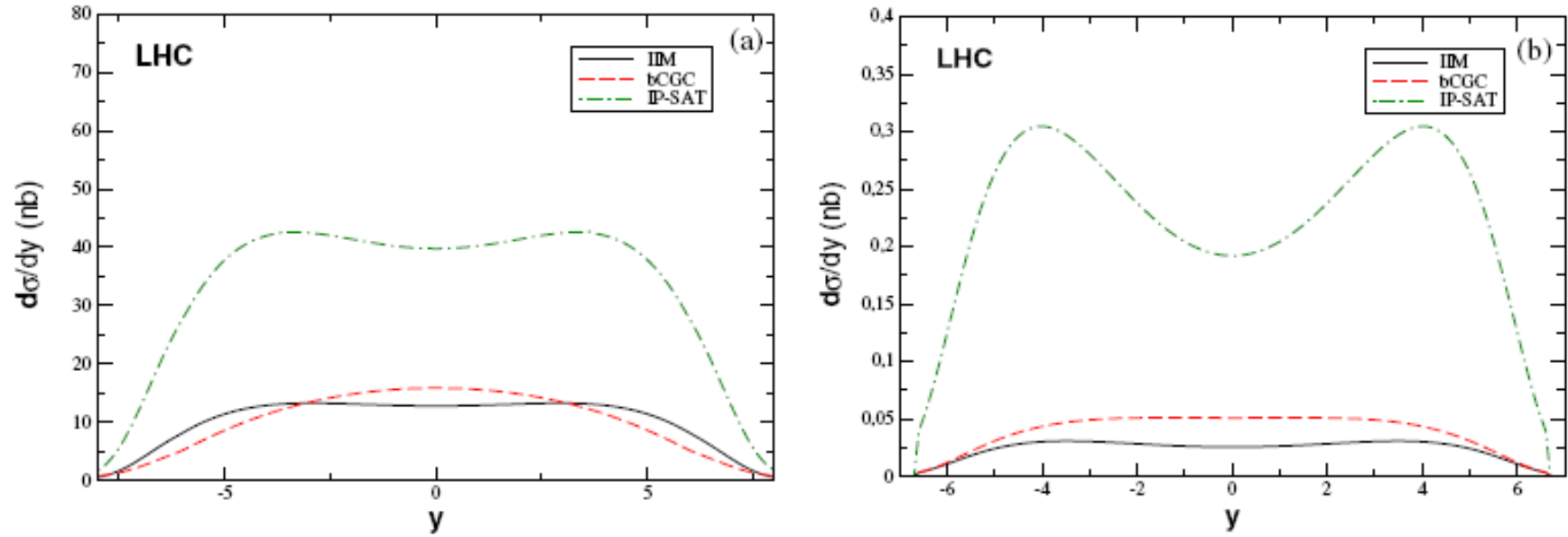


FIG. 6 (color online). The rapidity distribution for the diffractive charm (left panel) and bottom (right panel) photoproduction on $p\bar{p}$ reactions at LHC energy $\sqrt{s_{NN}} = 14$ TeV. Different curves correspond to distinct phenomenological models.

Heavy quark photoproduction in coherent interactions at high energiesV. P. Gonçalves,¹ M. V. T. Machado,² and A. R. Meneses¹TABLE I. The integrated cross section for the inclusive and diffractive photoproduction of heavy quarks in $pp(\bar{p})$ collisions at Tevatron and LHC energies.

	$Q\bar{Q}$	IIM	bCGC	IP-SAT
Tevatron	$c\bar{c}$ (inclusive)	1230 nb	1245 nb	2310 nb
	$c\bar{c}$ (diffractive)	37 nb	49 nb	114 nb
	$b\bar{b}$ (inclusive)	11 nb	10 nb	32 nb
	$b\bar{b}$ (diffractive)	0.04 nb	0.08 nb	0.30 nb
LHC	$c\bar{c}$ (inclusive)	3821 nb	3662 nb	7542 nb
	$c\bar{c}$ (diffractive)	165 nb	161 nb	532 nb
	$b\bar{b}$ (inclusive)	51 nb	51 nb	158 nb
	$b\bar{b}$ (diffractive)	0.32 nb	0.52 nb	3 nb

Coherent interactions as a probe of the Pomeron

PHYSICAL REVIEW D 85, 054019 (2012)

Heavy quark production in $\gamma\mathbb{P}$ interactions at hadronic colliders

V. P. Gonçalves and M. M. Machado

$$\begin{aligned}\sigma(\gamma h \rightarrow Q\bar{Q}Xh)(W_{\gamma h}) \\ &= \int_{x_{\min}}^1 dx \sigma^{\gamma g \rightarrow Q\bar{Q}}(W_{\gamma g}) g^D(x, \mu^2), \\ g^D(x, \mu^2) &= \int dx_{\mathbb{P}} d\beta \delta(x - x_{\mathbb{P}}\beta) g_{\mathbb{P}}(\beta, \mu^2) f_{\mathbb{P}}(x_{\mathbb{P}}) \\ &= \int_x^1 \frac{dx_{\mathbb{P}}}{x_{\mathbb{P}}} f_{\mathbb{P}}(x_{\mathbb{P}}) g_{\mathbb{P}}\left(\frac{x}{x_{\mathbb{P}}}, \mu^2\right),\end{aligned}$$

TABLE II. Comparison between the total cross sections for the inclusive and diffractive charm and bottom photoproduction in pp and pPb collisions at LHC.

		Inclusive	Diffractive dipole model	Diffractive resolved Pomeron
Charm	pp	6697 nb	161 nb	1208 nb
	pPb	5203 μb	145 μb	694 μb
Bottom	pp	123 nb	0.52 nb	15 nb
	pPb	55 μb	0.2 μb	4.5 μb

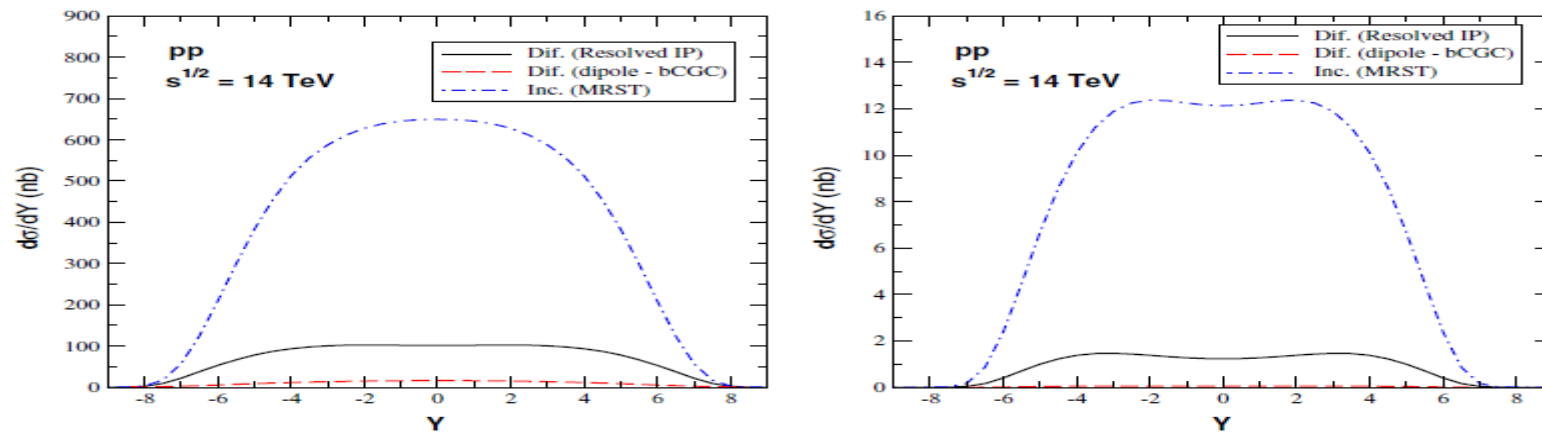


FIG. 2 (color online). Rapidity distribution for the inclusive and diffractive charm (left panel) and bottom (right panel) photoproduction in pp collisions at $\sqrt{s} = 14$ TeV.

Coherent interactions as a probe of the BFKL Pomeron

PHYSICAL REVIEW D 81, 074028 (2010)

Diffractive J/Ψ photoproduction at large momentum transfer in coherent hadron-hadron interactions at CERN LHC

V. P. Gonçalves* and W. K. Sauter†

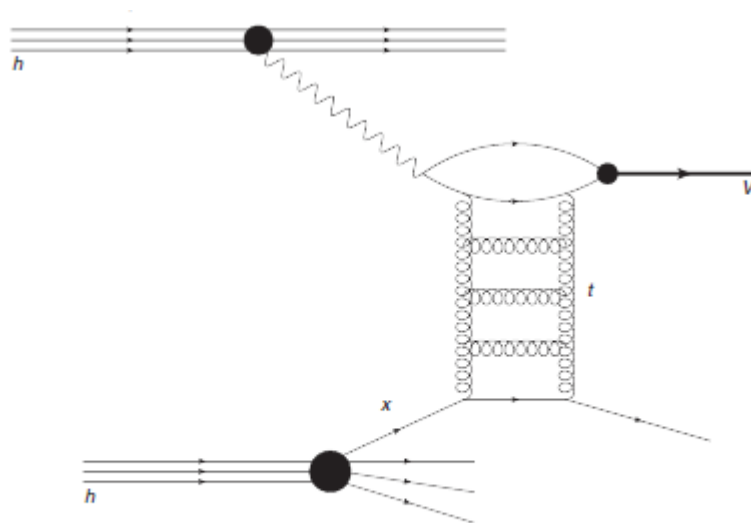


FIG. 1. High- t vector meson photoproduction in coherent hadron-hadron collisions.

Coherent interactions as a probe of the BFKL Pomeron

PHYSICAL REVIEW D 81, 074028 (2010)

Diffractive J/Ψ photoproduction at large momentum transfer in coherent hadron-hadron interactions at CERN LHC

V. P. Gonçalves* and W. K. Sauter†

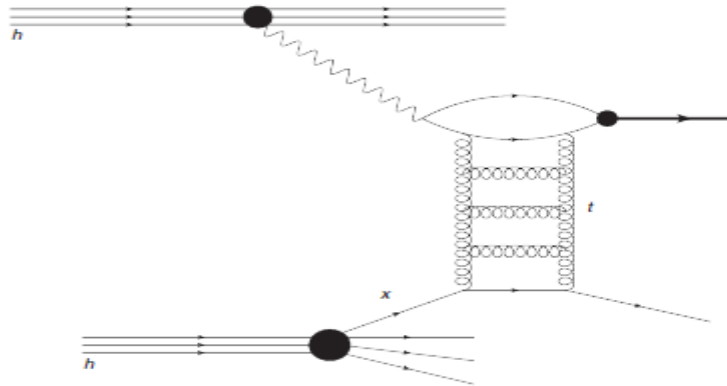


FIG. 1. High- t vector meson photoproduction in coherent hadron-hadron collisions.

$$\frac{d\sigma[h_1 + h_2 \rightarrow h_1 \otimes J/\Psi \otimes X]}{dydt} = \omega \frac{dN_\gamma(\omega)}{d\omega} \frac{d\sigma_{\gamma h \rightarrow J/\Psi X}}{dt}(\omega),$$

$$\frac{d\sigma(\gamma h \rightarrow VX)}{dtdx_j} = \left[\frac{81}{16} G(x_j, |t|) + \sum_j (q_j(x_j, |t|) + \bar{q}_j(x_j, |t|)) \right] \frac{d\sigma(\gamma q \rightarrow Vq)}{dt},$$

$$\frac{d\sigma(\gamma q \rightarrow J/\Psi q)}{dt} = \frac{16\pi}{81t^4} |\mathcal{F}(z, \tau)|^2.$$

* The BFKL amplitude, in the LLA and lowest conformal spin ($n = 0$), is given by [36]

$$\mathcal{F}_{\text{BFKL}}(z, \tau) = \frac{t^2}{(2\pi)^3} \int d\nu \frac{\nu^2}{(\nu^2 + 1/4)^2} e^{\chi(\nu)z} I_\nu^{J/\Psi}(Q_\perp) \times I_\nu^{q\bar{q}}(Q_\perp)^*, \quad (11)$$

where Q_\perp is the momentum transferred, $t = -Q_\perp^2$ (the subscript denotes two-dimensional transverse vectors), and

$$\chi(\nu) = 4\text{Re}(\psi(1) - \psi(\frac{1}{2} + i\nu)) \quad (12)$$

is proportional to the BFKL kernel eigenvalues [39] with $\psi(x)$ being the digamma function.

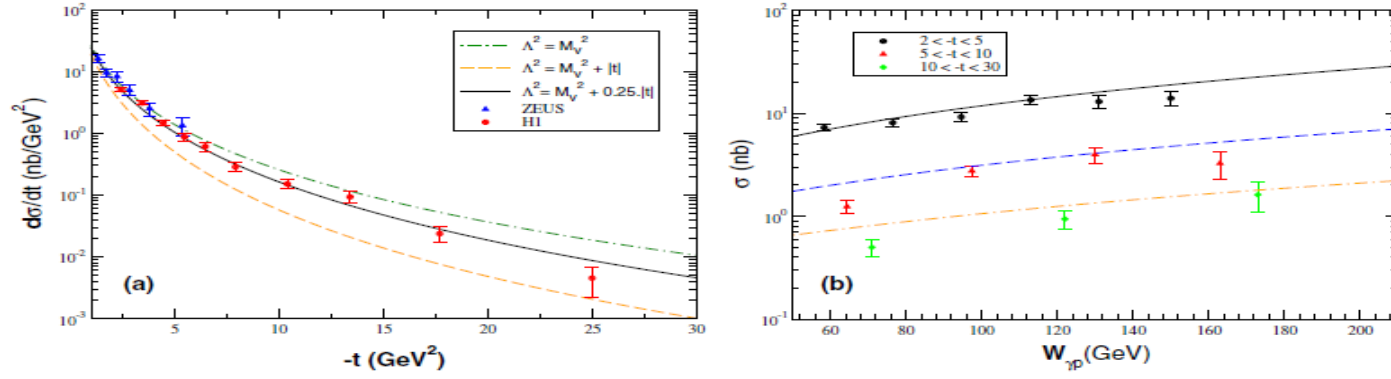


FIG. 2 (color online). (a) Differential cross section for J/Ψ production: theory compared to HERA data ($\langle W \rangle = 100$ GeV). (b) Energy dependence of the total cross section for distinct t ranges. Data are from H1 [41] and ZEUS [42] Collaborations.

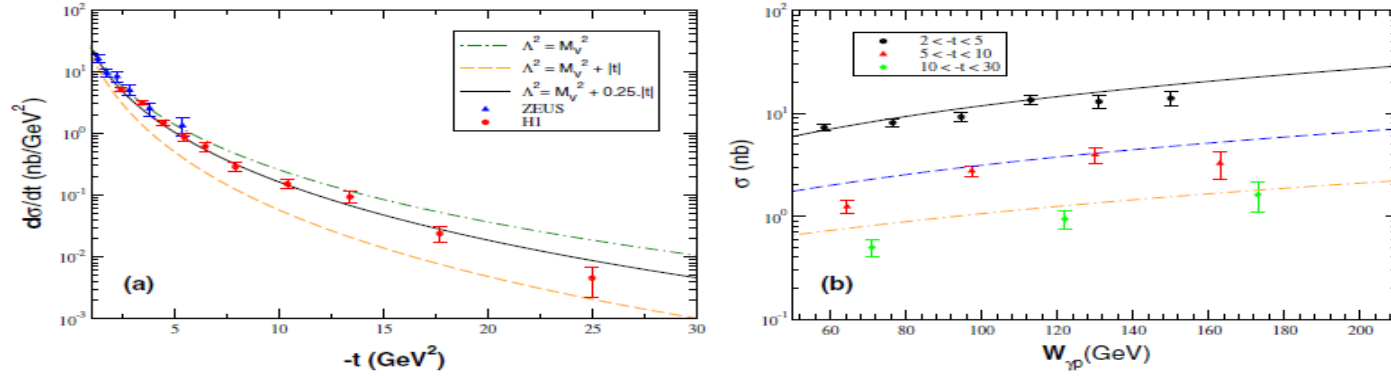


FIG. 2 (color online). (a) Differential cross section for J/Ψ production: theory compared to HERA data ($\langle W \rangle = 100$ GeV). (b) Energy dependence of the total cross section for distinct t ranges. Data are from H1 [41] and ZEUS [42] Collaborations.

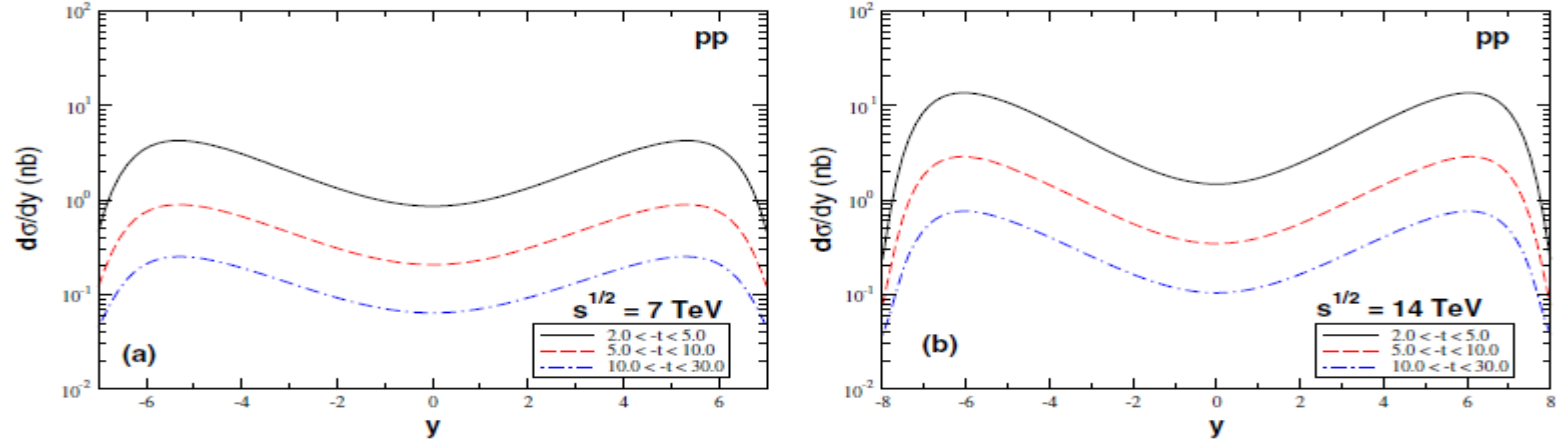


FIG. 4 (color online). Rapidity distribution for the diffractive J/Ψ photoproduction in pp collisions at LHC for distinct t ranges and different values of the center-of-mass energy: (a) $\sqrt{s} = 7.0$ TeV, and (b) $\sqrt{s} = 14.0$ TeV.

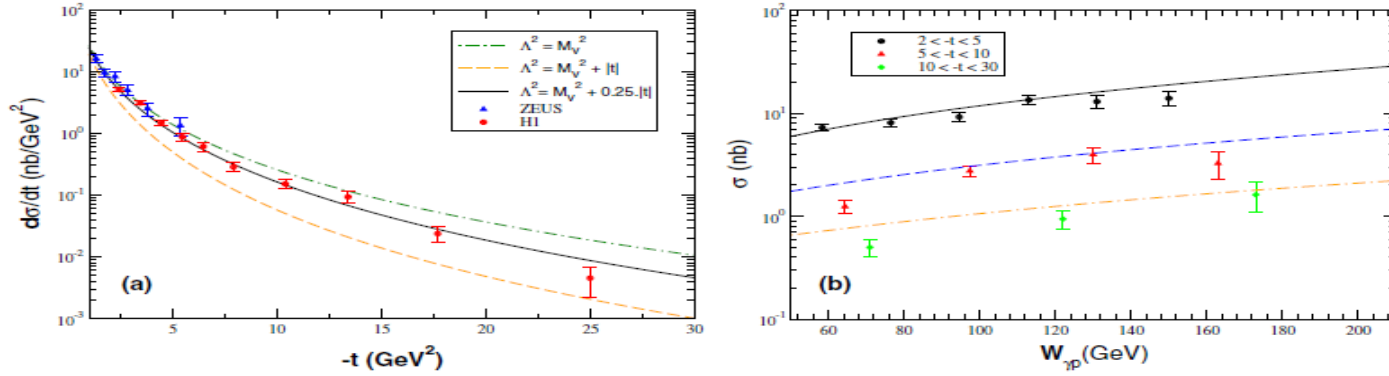


FIG. 2 (color online). (a) Differential cross section for J/Ψ production: theory compared to HERA data ($\langle W \rangle = 100$ GeV). (b) Energy dependence of the total cross section for distinct t ranges. Data are from H1 [41] and ZEUS [42] Collaborations.

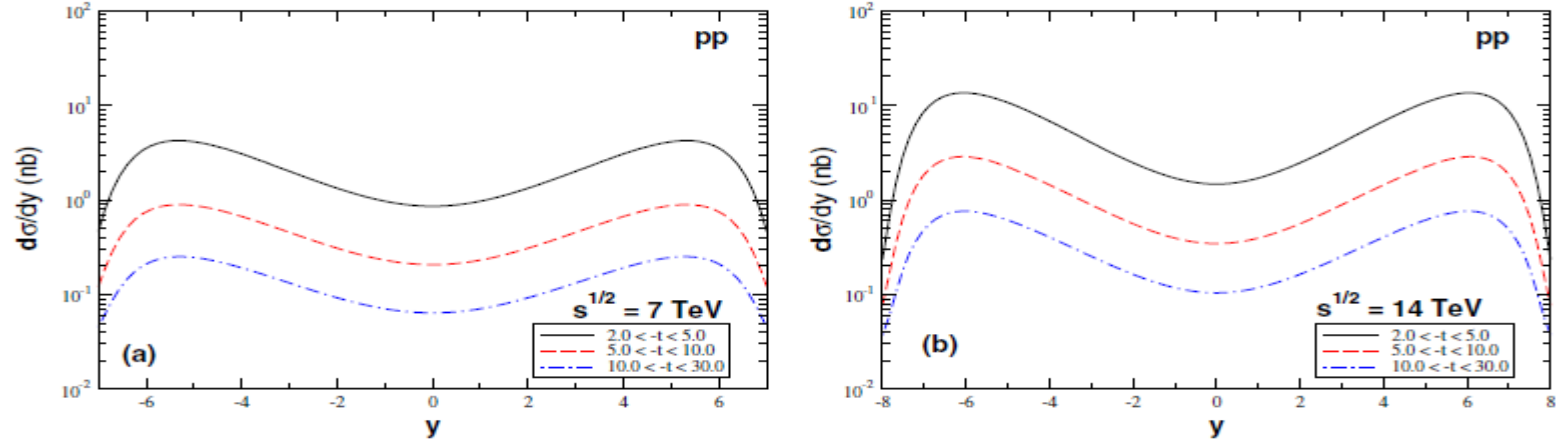


FIG. 4 (color online). Rapidity distribution for the diffractive J/Ψ photoproduction in pp collisions at LHC for distinct t ranges and different values of the center-of-mass energy: (a) $\sqrt{s} = 7.0$ TeV, and (b) $\sqrt{s} = 14.0$ TeV.

TABLE I. The integrated cross section (event rates/second) for the diffractive J/Ψ photoproduction at large momentum transfer in pp and AA collisions at LHC.

	pp ($\sqrt{s} = 7$ TeV)	pp ($\sqrt{s} = 14$ TeV)	$PbPb$ ($\sqrt{s} = 5.5$ TeV)
$2.0 < t < 5.0$	320 nb (320.0)	970 nb (970.0)	30 mb (13.0)
$5.0 < t < 10.0$	70 nb (70.0)	210 nb (210.0)	09 mb (0.38)
$10.0 < t < 30.0$	20 nb (20.0)	60 nb (60.0)	03 mb (0.12)

Diffractive vector meson production at large t in coherent hadronic interactions at CERN LHC

V.P. Gonçalves^a and W.K. Sauter^b

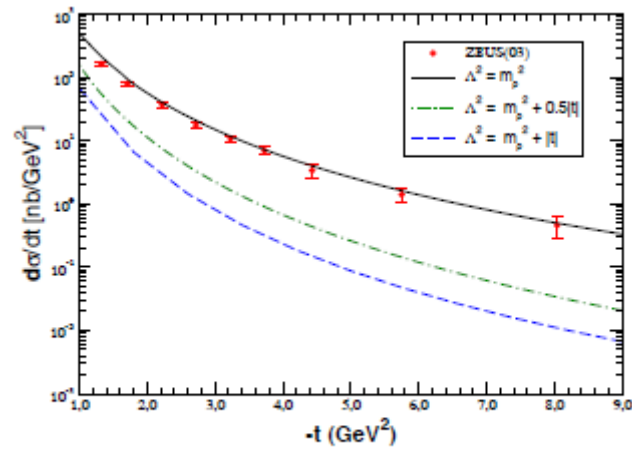
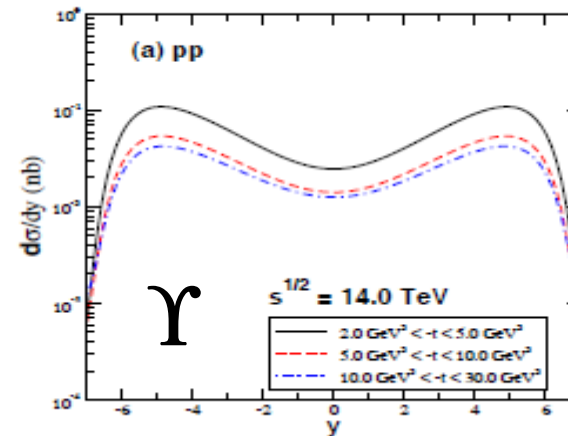
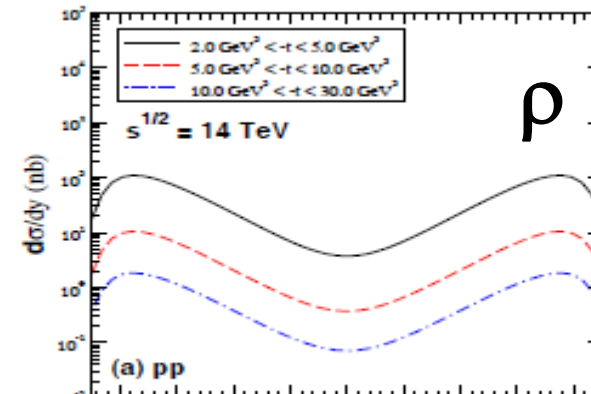


Fig. 1. (Color online) Differential cross-section for high- t diffractive ρ photoproduction. Data from ref. [27].



Coherent interactions as a probe of the Odderon

Probing the Odderon in coherent hadron - hadron interactions at CERN LHC

V. P. Gonçalves*

*High and Medium Energy Group,
Instituto de Física e Matemática,
Universidade Federal de Pelotas*

Caixa Postal 354, CEP 96010-900, Pelotas, RS, Brazil

(Dated: November 7, 2012)

arXiv: 1211.1207

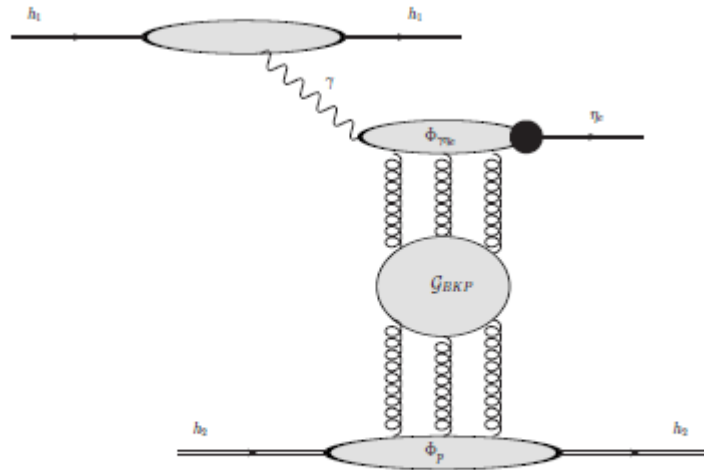


FIG. 1: Illustration of the coherent process $h_1 + h_2 \rightarrow h_1 h_2 \eta_c$ (See text).

In this paper we propose the study of the diffractive η_c photoproduction in coherent interactions as a new alternative to probe the Odderon in pp and $PbPb$ collisions at CERN - LHC. As the Pomeron exchange cannot contribute to this process, its observation would indicate the existence of the Odderon. We predict total cross sections of order of $pb(\mu b)$ for $pp(PbPb)$ collisions and large values for the event rates/year, which makes, in principle, the experimental analysis of this process feasible at LHC.

$\sqrt{s_{NN}}$	CKMS	BBCV
8 TeV	0.55 pb (55000)	10.10 pb (1×10^6)
14 TeV	0.65 pb (65000)	13.90 pb (1.4×10^6)

TABLE I: Cross sections (event rates/year) for the diffractive η_c photoproduction in pp collisions at LHC energies.

$\sqrt{s_{NN}}$	CKMS	BBCV
2.76 TeV	0.30 μb (126)	14.25 μb (5985)
5.5 TeV	0.40 μb (168)	23.59 μb (9912)

TABLE II: Cross sections (event rates/year) for the diffractive η_c photoproduction in $PbPb$ collisions at LHC energies.

Summary

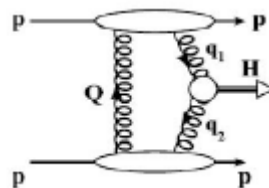
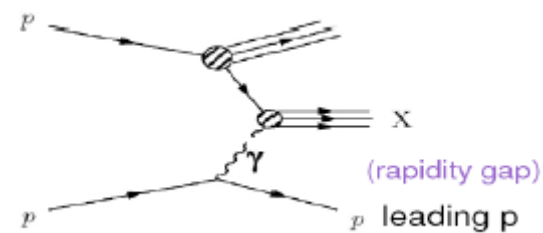
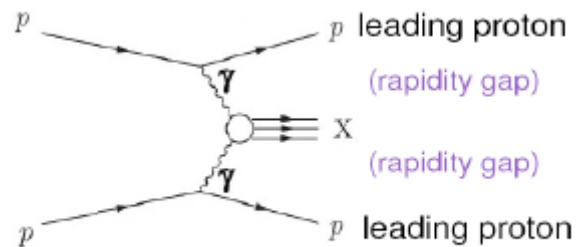
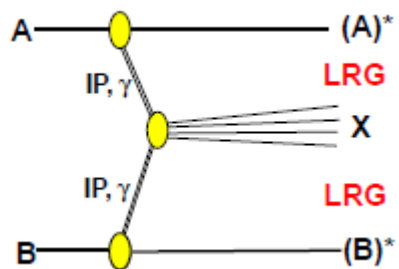
- ✓ The study of the inclusive and exclusive photoproduction of different final states at LHC can be useful to constrain the QCD dynamics;
- ✓ **Main challenge:** Experimental separation of the photon – hadron interactions.
- In general, the corresponding cross sections are smaller than those for the production of the same final states in pomeron – pomeron (HQ, VM) or photon – photon interactions (η_c).
- **One possibility:** Measurement of the transverse momentum of the scattered hadrons.

Summary

- ✓ The study of the inclusive and exclusive photoproduction of different final states at LHC can be useful to constrain the QCD dynamics;
- ✓ **Main challenge:** Experimental separation of the photon – hadron interactions.
- ❑ In general, the corresponding cross sections are smaller than those for the production of the same final states in pomeron – pomeron (HQ, VM) or photon – photon interactions (η_c).
- ❑ **One possibility:** Measurement of the transverse momentum of the scattered hadrons.

Thank you !

Extra slides



Quarkonium+ γ production in coherent hadron–hadron interactions at LHC energies

V.P. Gonçalves^{1,a}, M.M. Machado²

$$\begin{aligned} & \frac{d\sigma[p + p \rightarrow p \otimes H + \gamma + X]}{dY} \\ &= \omega \frac{dN_{\gamma/h_1}(\omega)}{d\omega} \sigma_{\gamma h_2 \rightarrow H + \gamma + X}(\omega) \\ &+ \omega \frac{dN_{\gamma/h_2}(\omega)}{d\omega} \sigma_{\gamma h_1 \rightarrow H + \gamma + X}(\omega), \end{aligned}$$

$$\begin{aligned} & \sigma(\gamma + p \rightarrow H + \gamma + X) \\ &= \int dz dp_{\perp}^2 \frac{xg(x, Q^2)}{z(1-z)} \frac{d\sigma}{dt}(\gamma + g \rightarrow H + \gamma) \end{aligned}$$

$$\begin{aligned} & \frac{d\sigma}{dt}(\gamma + g \rightarrow H + \gamma) \\ &= \frac{64\pi^2}{3} \frac{e_Q^4 \alpha^2 \alpha_s m_Q}{s^2} \left(\frac{s^2 s_1^2 + t^2 t_1^2 + u^2 u_1^2}{s_1^2 t_1^2 u_1^2} \right) \langle O_8^V(^3S_1) \rangle \end{aligned}$$

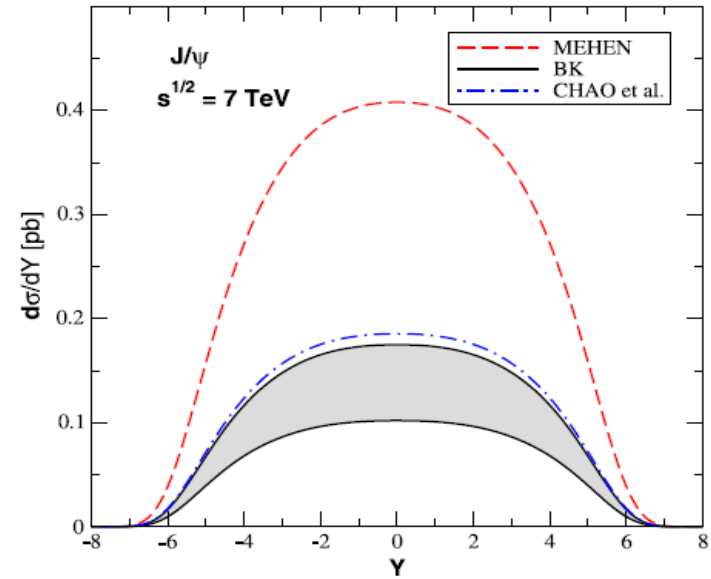


Table 1 The total cross section for the $H + \gamma$ photoproduction in coherent hadron–hadrons collisions at LHC energies

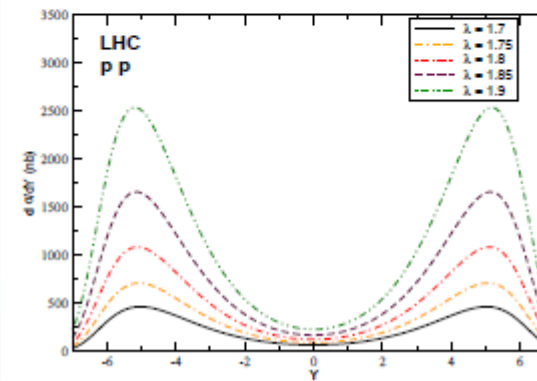
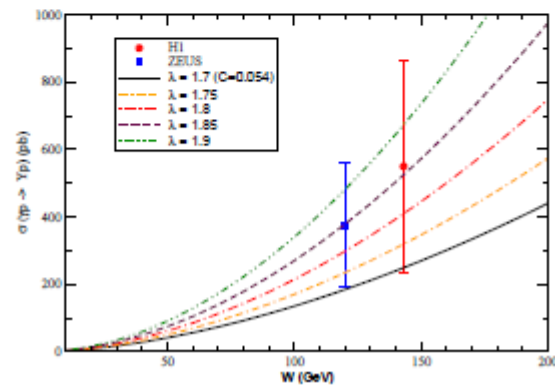
$J/\psi + \gamma$	MEHEN	BK
LHC (7 TeV)	3.62 pb	1.23 ± 0.50 pb
LHC (14 TeV)	5.60 pb	1.90 ± 0.32 pb
$\gamma + \gamma$	BFL	BSV
LHC (14 TeV)	5.46 fb	1.45 ± 0.13 fb

Constraining the growth of the cross section

At leading order

$$\frac{d\sigma(\gamma h \rightarrow Vh)}{dt} \Big|_{t=0} = \frac{\pi^3 \Gamma_{ee} M_V^3}{48\alpha} \frac{\alpha_s^2(\overline{Q}^2)}{\overline{Q}^8} \times [xg_h(x, \overline{Q}^2)]^2 ,$$

where xg_h is the target gluon distribution, $x = 4\overline{Q}^2/W^2$ with W the center of mass energy and $\overline{Q}^2 = M_V^2/4 \Rightarrow \sigma(\gamma h \rightarrow Vh) \propto W^\lambda$



Coherent photon-hadron interactions in pA collisions: Small- x physics after HERA

V. P. Gonçalves¹ and M. V. T. Machado^{2,3}

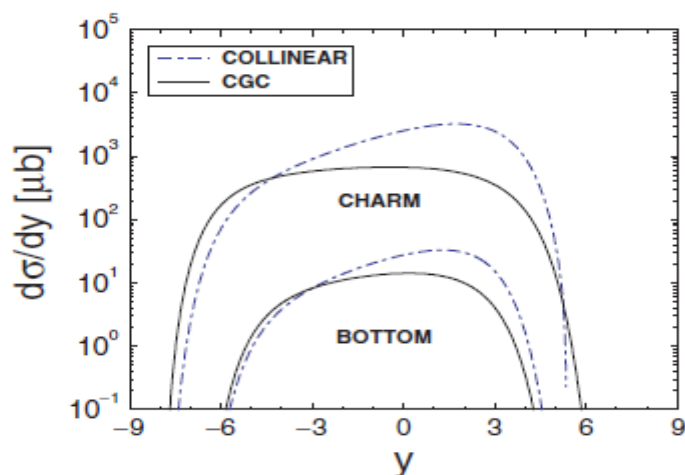


FIG. 1. (Color online) Rapidity distribution for heavy quark photoproduction on pA reactions for LHC energy (see text).

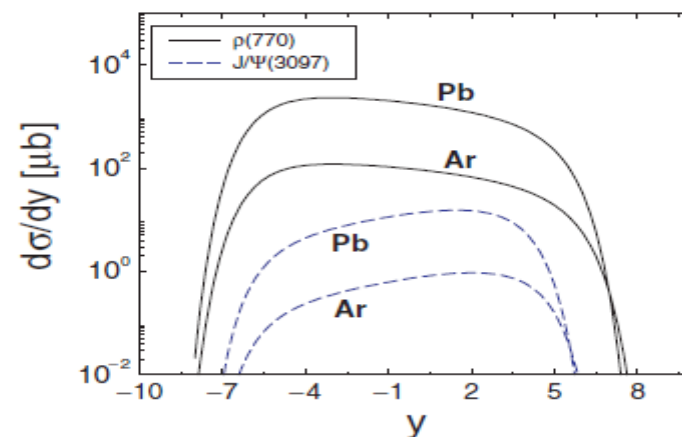


FIG. 2. (Color online) Rapidity distribution for vector meson photoproduction on pA reactions at LHC energy (see text).

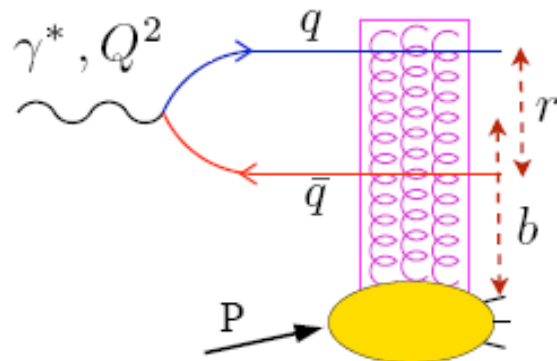
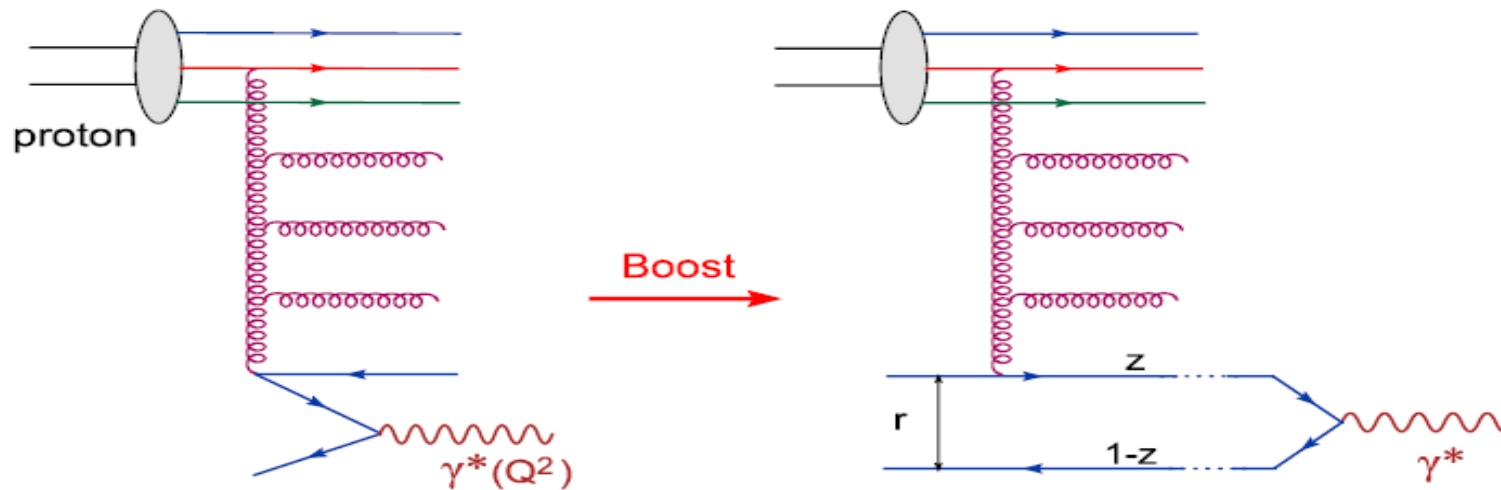
TABLE I. The integrated cross section (event rates/month) for the photoproduction of heavy quarks and vector mesons in pA collisions at LHC (see text).

	X	COLLINEAR	CGC
LHC	$c\bar{c}$	17 mb (10^{10})	5 mb (1×10^9)
	$b\bar{b}$	155 μ b (10^8)	81 μ b (6×10^7)
	ρ	—	14 mb (1×10^{10})
	J/ψ	—	95 μ b (7×10^7)

QCD dynamics at high energies

- Lorentz boost to the 'dipole frame'

γ^* fluctuates into a $q\bar{q}$ pair which then scatters off the proton.



$$\sigma_{T,L}^{\gamma^* P}(x, Q^2) = \int_0^1 dz \int d^2 \mathbf{r} \left| \Psi_{T,L}^{\gamma^* \rightarrow q\bar{q}}(z, Q, r) \right|^2 \sigma^{dip}(x, r)$$

$$\sigma^{dip}(x, r) = 2 \int d^2 b \mathcal{N}(x, b, r) \rightarrow \text{Dipole cross section. Strong interactions and x-dependence are here}$$

QCD dynamics at high energies

Inclusive deep-inelastic scattering (DIS) at small x

$$\begin{aligned}\sigma_{T,L}^{\gamma^*P}(x, Q) &= \text{Im } \mathcal{A}_{T,L}^{\gamma^*P \rightarrow \gamma^*P}(x, Q, \Delta = 0) \\ &= \sum_f \int d^2\mathbf{r} \int_0^1 \frac{dz}{4\pi} (\Psi^* \Psi)_{T,L}^f \int d^2\mathbf{b} \frac{d\sigma_{q\bar{q}}}{d^2\mathbf{b}}\end{aligned}$$

Exclusive diffractive processes

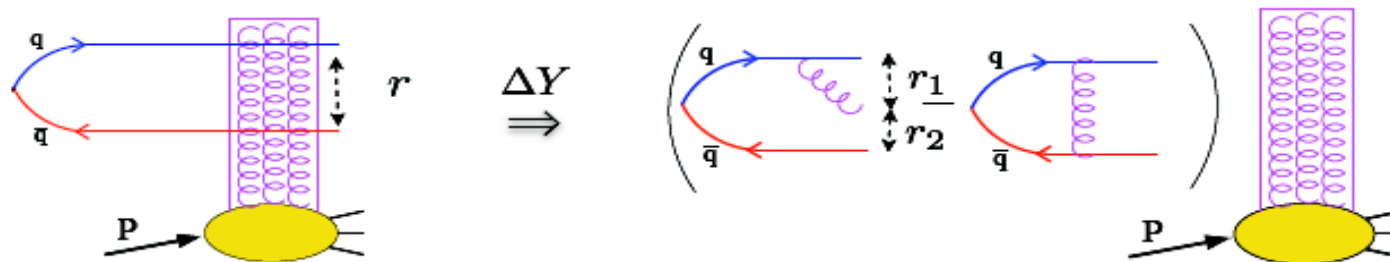
$$\frac{d\sigma_{T,L}^{\gamma^*P \rightarrow Ep}}{dt} = \frac{1}{16\pi} \left| \mathcal{A}_{T,L}^{\gamma^*P \rightarrow Ep} \right|^2$$

$$\mathcal{A}_{T,L}^{\gamma^*P \rightarrow Ep}(x, Q, \Delta) = i \int d^2\mathbf{r} \int_0^1 \frac{dz}{4\pi} \int d^2\mathbf{b} (\Psi_E^* \Psi)_{T,L} e^{-i[\mathbf{b} - (1-z)\mathbf{r}] \cdot \Delta} \frac{d\sigma_{q\bar{q}}}{d^2\mathbf{b}}$$

$$\frac{d\sigma_{q\bar{q}}}{d^2\mathbf{b}} = 2 \mathcal{N}(x, r, b), \text{ where } \mathcal{N} \in [0, 1] \text{ and } \mathcal{N} = 1 \text{ is the unitarity limit.}$$

QCD dynamics at high energies

⇒ **pQCD tools:** The non-linear **Balitsky-Kovchegov eqn.** describes the small- x evolution of the dipole scattering amplitude at leading order in $\alpha_s \ln(1/x)$



$$\frac{\partial \mathcal{N}(x, r)}{\partial \ln(x_0/x)} = \int d^2 r_1 K^{LO}(\mathbf{r}, \mathbf{r}_1, \mathbf{r}_2) [\mathcal{N}(x, r_1) + \mathcal{N}(x, r_2) - \mathcal{N}(x, r) - \mathcal{N}(x, r_1)\mathcal{N}(x, r_2)]$$

The LL kernel: $K^{LO}(\mathbf{r}, \mathbf{r}_1, \mathbf{r}_2) = \frac{\alpha_s N_c}{2\pi^2} \frac{r^2}{r_1^2 r_2^2}$

↑
Non-linear term

⇒ **However,** at LL accuracy (fixed coupling) the BK equation is not compatible with data

$$\left\{ \begin{array}{l} Q_s^2(Y) = Q_0^2 \exp \lambda Y \\ \lambda = \frac{d \ln Q_s^2(Y)}{dY} \end{array} \right.$$

**Fits to HERA
and RHIC data**

$$\lambda \sim 0.2 \div 0.3$$

**LL-BK
(fixed coupling)**

$$\lambda^{LL} \sim 4.8 \alpha_s$$

Phenomenological models:

$\frac{d\sigma_{q\bar{q}}}{d^2\mathbf{b}} = 2 \mathcal{N}(x, r, b)$, where $\mathcal{N} \in [0, 1]$ and $\mathcal{N} = 1$ is the unitarity limit.

- Most dipole models assume a factorised b dependence:

$$\mathcal{N}(x, r, b) = T(b) \mathcal{N}(x, r), \quad \text{with } \mathcal{N}(x, r) \in [0, 1],$$

e.g. $T(b) = \Theta(R_p - b)$, so that the b -integrated $\sigma_{q\bar{q}}$ is

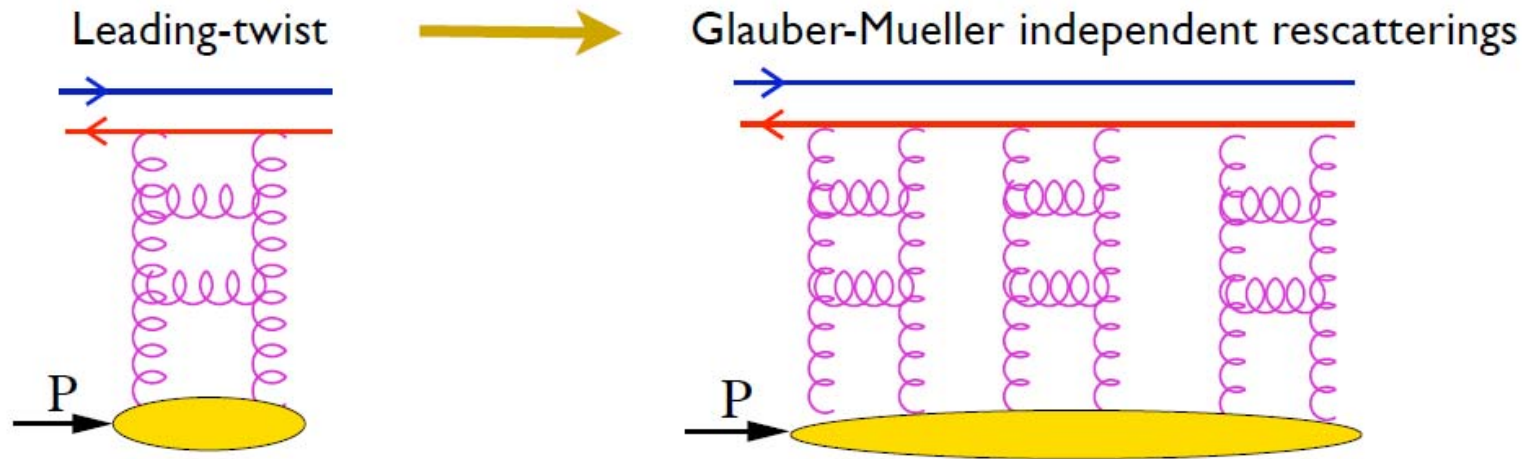
$$\sigma_{q\bar{q}} = 2 \int d^2\mathbf{b} \mathcal{N}(x, r, b) = 2 \int d^2\mathbf{b} T(b) \mathcal{N}(x, r) = \sigma_0 \mathcal{N}(x, r).$$

Golec-Biernat-Wustoff:

$$\mathcal{N}^{GBW}(x, b, r) = \theta(R_p - b) \left(1 - \exp \left[-\frac{r^2 Q_s^2(x)}{4} \right] \right)$$

$$Q_s^2(x) = Q_{s0}^2 \left(\frac{x_0}{x} \right)^\lambda \quad \text{with} \quad \lambda \sim 0.2 \div 0.3$$

Impact parameter dependent saturation model (IP-SAT)



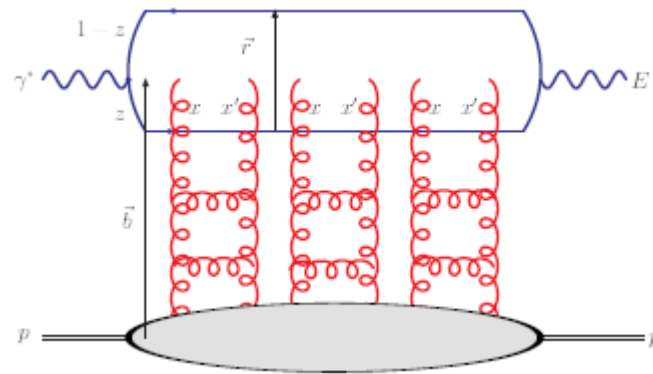
$$\frac{d\sigma^{dip}}{d^2b} \sim \frac{\pi^2}{2N_c} r^2 xg(x, Q^2) T_p(b)$$

$$\frac{d\sigma^{dip}}{d^2b} = 1 - \exp \left[-\frac{\pi^2}{2N_c} r^2 xg(x, Q^2) T_p(b) \right]$$

Leading $\ln Q^2$ terms in each cascade resummed through DGLAP

All the Bjorken- x dependence is encoded in that of the gluon distribution.

Impact parameter dependent saturation model (IP-SAT)



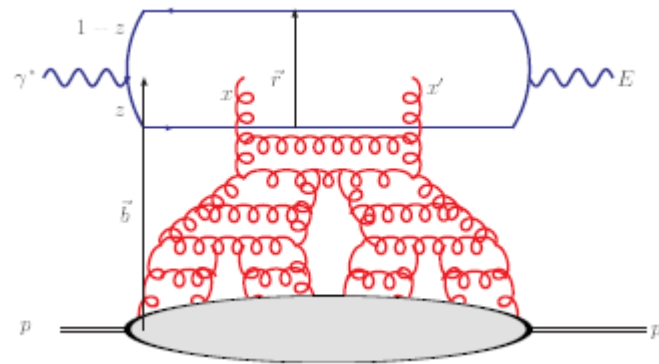
- Eikonalised DGLAP-evolved gluon density with Gaussian b dependence:

$$\mathcal{N}(x, r, b) = 1 - \exp \left(-\frac{\pi^2}{2N_c} r^2 \alpha_S(\mu^2) xg(x, \mu^2) T(b) \right)$$

$$xg(x, \mu_0^2) = A_g x^{-\lambda_g} (1-x)^{5.6}, \quad T(b) = \frac{1}{2\pi B_G} e^{-\frac{b^2}{2B_G}}, \quad \mu^2 = \frac{4}{r^2} + r_0^2$$

- $B_G = 4 \text{ GeV}^{-2}$ from t -slope of exclusive J/ψ photoproduction.
- Fit to 163 ZEUS F_2 points with $x_{Bj} \leq 0.01$ and $Q^2 \in [0.25, 650] \text{ GeV}^2$ gives a $\chi^2/\text{d.o.f.} = 1.21$ with parameters:
 $\mu_0^2 = 1.17 \text{ GeV}^2$, $A_g = 2.55$, $\lambda_g = 0.020$.

Impact parameter dependent CGC model (b-CGC)

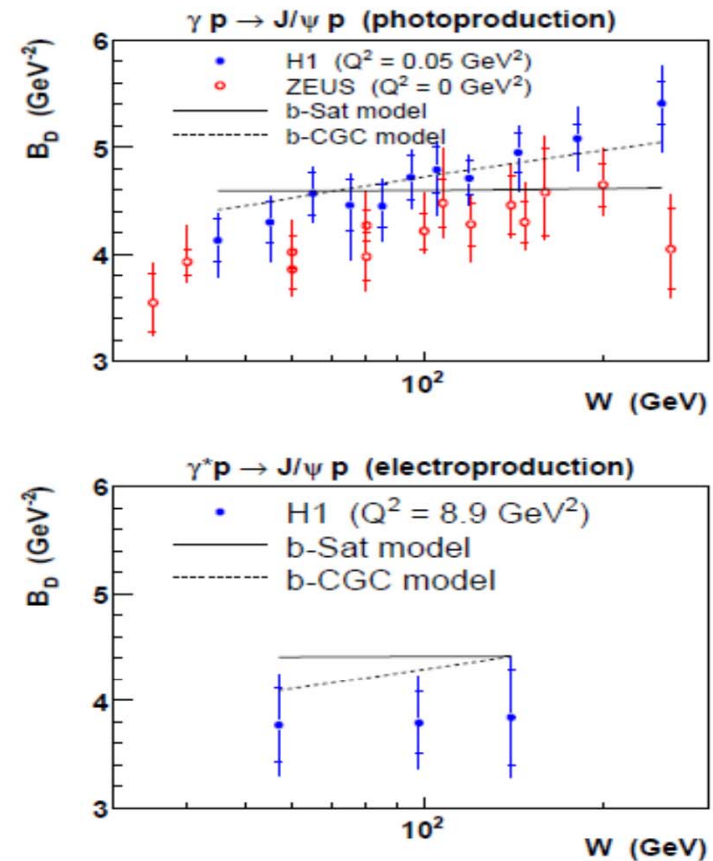
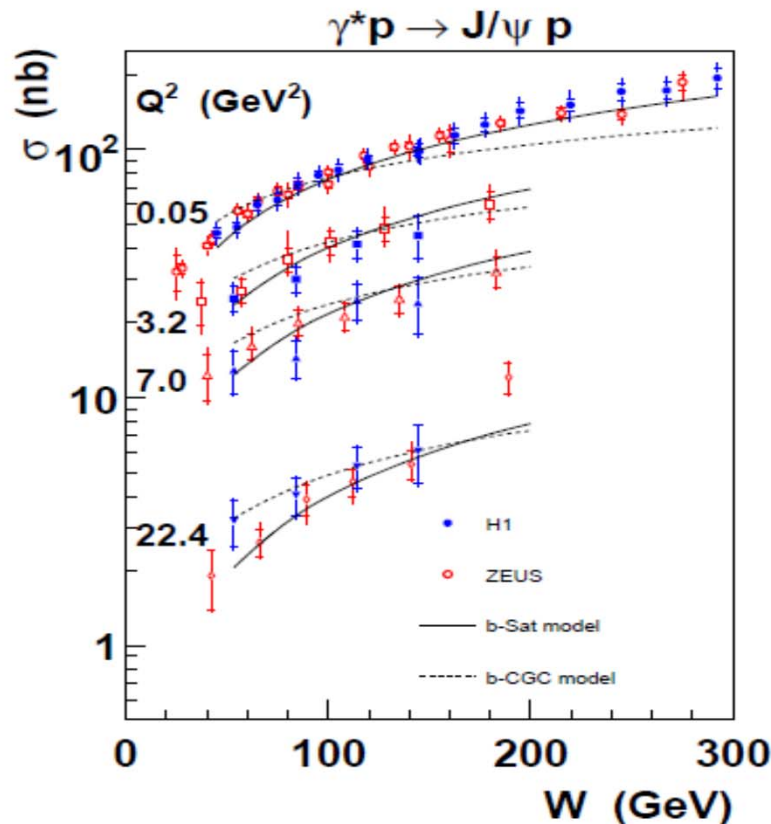


- Approximate solution of the Balitsky–Kovchegov (BK) equation.
- Original colour glass condensate (CGC) model of [Iancu, Itakura and Munier](#) assumed a factorised b dependence, $\Theta(R_p - b)$.
- Introduce b dependence into the saturation scale:

$$\mathcal{N}(x, r, b) = \begin{cases} \mathcal{N}_0 \left(\frac{rQ_s}{2} \right)^{2\left(\gamma_s + \frac{\ln(2/rQ_s)}{9.9\lambda \ln(1/x)}\right)} & : rQ_s \leq 2 \\ 1 - e^{-A \ln^2(BrQ_s)} & : rQ_s > 2 \end{cases}$$

$$Q_s \equiv Q_s(x, b) = \left(\frac{x_0}{x} \right)^{\frac{\lambda}{2}} \left[\exp \left(-\frac{b^2}{2B_{\text{CGC}}} \right) \right]^{\frac{1}{2\gamma_s}}$$

Exclusive J/ψ photoproduction at HERA



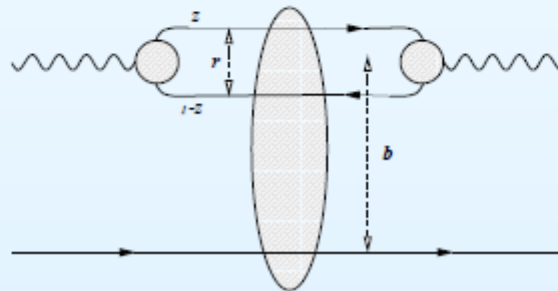
- W dependence of J/ψ photoproduction favours b-Sat model.
- Slope of B_D (t -slope) vs. W , i.e. $\alpha'_{\mathbb{P}}$, favours b-CGC model.

Heavy Quark Photoproduction: The Dipole approach

Considering γh scattering in the dipole model, the probing projectile fluctuates into a quark-antiquark pair (a dipole) with transverse separation r long after the interaction, which then scatters off the proton. The $Q\bar{Q}$ production cross section reads as,

$$\sigma(\gamma h \rightarrow Q\bar{Q}X) = \sum_{i=T,L} \int dz d^2r \Psi_i^\gamma(z, r, Q^2) \sigma_{dip}(x, r) \Psi_i^{\gamma*}(z, r, Q^2)$$

- The basic blocks are the photon wavefunction, Ψ^γ and the dipole-target cross section, σ_{dip} .



$\text{Pb+Pb} \rightarrow \text{Pb+Pb+J}/\psi \quad \sqrt{s_{\text{NN}}} = 2.76 \text{ TeV}$

